UC Santa Barbara
Recent Work

Title

Derivation of the Viscous Moore-Greitzer Equation for Aeroengine Flow

Permalink

https://escholarship.org/uc/item/8sk0b2q4

Authors

Birnir, Bjorn
Hou, Songming
Wellander, Niklas

Publication Date

2007

Derivation of the Viscous Moore-Greitzer Equation for Aeroengine Flow

Björn Birnir [*]   Songming Hou [†]   Niklas Wellander [‡]

Keywords: Separation of scales, scaling, modeling, homogenization, two-scale convergence, compressor, jet engine flow.

AMS classification numbers: 34D45, 34K15, 35B27, 35B40, 74Q15, 76M50

Abstract

The viscous Moore-Greitzer equation modeling the airflow through the compression system in turbomachines, such as a jet engine, is derived using a scaled Navier-Stokes equation. The method utilizes a separation of scales argument, based on the different spatial scales in the engine and the different time scales in the flow. The pitch and size of the rotor-stator pair of blades provides a small parameter, which is the size of the local cell. The motion of the stator and rotor blades in the compressor produces a very turbulent flow on a fast time scale. The leading order equation, for the fast-time and local scale, describes this turbulent flow. The next order equations, produce an axi-symmetric swirl and a flow-pattern analogous to Rayleigh-Bénard convection rolls in Rayleigh-Bénard convection. On a much larger spatial scale and a slower time scale, there exist modulations of the flow including instabilities called surge and stall. A higher order equation, in the small parameter, describes these global flow modulations, when averaged over the small (local) spatial scales, the fast time scale and the time scale of the vortex rotations. Thus a more general system of spatially global, slow-time equations is obtained. This system can be solved numerically without any approximations. The viscous Moore- Greitzer equation is obtained when small inertial terms are dropped from these slow-time, spatially global equations, averaged once more in the axial direction. The new equations are simulated with two different simplifying assumptions and the results compared with simulations of the viscous Moore-Greitzer equations.

1   Introduction

In recent years a lot of attention has been devoted to the study of air flow and combustion in turbomachines. The main reason for this interest is that when a turbomachine, such as a jet engine, operates close to its optimal operating parameter values, the flow can become unstable. These instabilities put a large stress on the engine and in some cases the engine needs to be turned off in order to recover the original operation conditions. For this reason jet engines are currently operated away from their optimal operating parameter values increasing both fuel consumption and the engine weight.

A jet engine can be thought of as a compressor, where the incoming air from the inlet duct is compressed by alternating rings of rotating blades and stationary blades. The mixture of fuel and compressed air then goes through the outlet duct to the plenum, where it is ignited and the resulting combustion generates thrust that propels the aircraft. Subsequently the air goes out of the plenum through the throttle where the process in the compressor is reversed. The air turns rotor blades as it rushes out of the throttle and these blades turn the rotors in the compressor.

Figure 1 shows a cartoon of the jet engine. The compressor has a cylindrical shape with inner boundary being the hub and outer boundary being the casing. The flow of air enters the engine through the inlet duct, then it enters the compressor where the pressure rise takes place. The air exits the compressor through the outlet duct and subsequently enters the plenum, where the combustion takes place. Then finally the mixture of air and residual gases exit through the throttle.
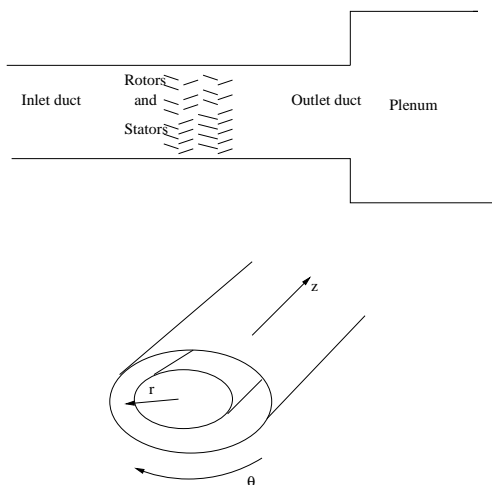

Figure 1: The jet engine

There are primarily two types of instabilities that occur in the flow through the compressor. They are called surge and stall. Surge is characterized by large oscillations of the mean mass flow through the engine. During part of the cycle, the mean mass flow

may become reversed, thrusting air out from the front of the engine. This puts a large stress on the components of the engine and seriously impairs its performance. When stall occurs, there are regions of relatively low air flow that form at isolated locations around the rim of the compressor. Here too, the phenomenon can be so pronounced that the flow in these isolated regions is reversed. Again this causes a large stress on the components of the engine and reduces its performance.

Moore and Greitzer published in 1986 a PDE model describing the airflow through the compression system in turbomachines, see [30], [31] and [13], and the earlier papers [27], [28], [29]. Although relatively simple, this model has been surprisingly successful at predicting experimental outcomes. Mezić [26] derived a model of the three dimensional flow in jet engine compressors. His model reduces to that presented in [5] and [8] when one assumes that the dependence of the flow on the radial direction is negligible. The viscous term in that equation, first introduced by Adomaitis and Abed [1], has however a new and better interpretation in Mezić's treatment. The term is not due to the viscosity of the air which is very small, but rather, it is a diffusion term due to the inviscid process of turbulent momentum transport via Reynolds stresses. The difference is a several orders of magnitude larger viscosity constant ν, which now represents the eddy viscosity. It is this model with the additional assumption that the flow has no radial component that will be compared to a homogenization limit of the Navier-Stoke equation below. In this guise the model is called the viscous Moore-Greitzer equation (vMG):

$$
\begin{cases}
\dfrac{\partial \varphi}{\partial t} &=& \nu \dfrac{\partial^2 \varphi}{\partial \theta^2} - \dfrac{1}{2}\dfrac{\partial \varphi}{\partial \theta} + \dfrac{1}{l_c}(\psi_c - \overline{\psi}_c) \\[2mm]
\dfrac{\partial \Phi}{\partial t} &=& \dfrac{1}{l_c}(\overline{\psi}_c - \Psi) \\[2mm]
\dfrac{\partial \Psi}{\partial t} &=& \dfrac{1}{4 l_c B^2}(\Phi - \gamma \, sgn(\Psi)\sqrt{|\Psi|})
\end{cases}
\tag{1.1}
$$

Here Φ is the mean flow (averaged over θ, in Figure 1) and φ is the deviation from the mean flow, Ψ is the pressure rise in the plenum, the compressor characteristic ψ_c is a force (pressure gradient) that is modeled as a cubic polynomial of $\Phi + \varphi$, $\overline{\psi}_c$ is the θ mean of ψ_c. To be more precise, the flow is the average over z of the velocity of air in the z direction, l_c is the total length of the inlet duct, the compressor and the outlet duct, B is a parameter expressing the geometry of the compressor and γ is the throttle parameter that is varied to open and close the throttle.

Thus the Moore-Greitzer model is a *continuum actuator disk model* for flow through discrete blade passages in the compressor. This means that we imagine the whole compressor cylinder being compressed into a disk, the actuator disk, that has the same effects on the flow as the compressor.

Birnir and Hauksson [5] proved the well-posedness and the existence of a finite dimensional attractor for the viscous Moore-Greitzer turbomachine model. They proved

that the Moore-Greitzer PDE model with viscosity has a unique solution in the Hilbert space $X = \overline{H}^1 \times \mathbf{R}^2$ where $\overline{H}^1$ denotes the Sobolev space, with index one, of functions on the unit circle with square integrable first derivative and zero mean. They also proved that this solution is smooth in space and time variables. Finally they proved that this dynamical system has a global attractor with finite Hausdorff and fractal dimensions and presented explicit estimates for the dimensions.

Banaszuk *et al.* [2] also considered the full PDE model of Moore and Greitzer. Chung and Titi [11] extended the analysis of Birnir and Hauksson [5] and proved that the viscous Moore-Greitzer possesses an inertial manifold and the solutions are (Gevrey) analytic. The estimates obtained in [5] on the dimensions of the attractor and the inertial manifolds are very large and not observed in numerical simulations, see [30], [25], [24], [7], [6] and [8]. Birnir and Hauksson [8] applied the theory of basic attractors [4] to get around this difficulty. The requirement that every point (function) of an attractor attracts a set of positive "infinite-dimensional" measure is much more restrictive than just to require a point to be attracting. Accordingly the basic attractors, the cores of the global attractors that possess this additional attractiveness, are low-dimensional whereas the global attractors themselves can in general be very high-dimensional, see [3].

Experimental, numerical and analytical results indicate that the stable solutions of the global attractor can be classified into the following groups: axisymmetric design flow (the desired operating flow) surge and stall. Surge has been fully analyzed in [30] and [25]. Stall was originally only analyzed in finite Galerkin approximations [30], [25], [24]. Birnir and Hauksson [7] gave a complete description of stall for a large parameter range. In this paper they analyzed stall, which is a part of the basic attractor forming the stable core of the global attractor. They showed that there can exist several stall solutions and analyzed their stability. They showed that only a small number of these solutions can be stable and belong to the basic attractor. This made it precise what qualitative information may be captured by such a Galerkin truncation of the solutions to the viscous Moore-Greitzer equations. Birnir and Hauksson [7] also provided the nonlinear stall modes that permit one to capture quantitative information about the solution and Xiao and Basar [36] found the center manifolds for the basic attractor components.

The final goal of all of the research discussed above was to understand the instabilities better in the framework of the viscous Moore-Greitzer partial differential equation and ultimately to produce control strategies for recovering design flow, after the system has been thrown into stall or surge. Banaszuk *et al.* [2] gave the first result in this direction, see also Humber and Krener [16], [17], and Xiao and Basar [35], but Birnir and Hauksson [6] and [8] were able to use their qualitative analysis of the basic attractor to develop optimal control of stall. This control strategy that has been implemented by Fontaine [12] may eventually lead to jet engine design which is lighter and more fuel efficient.

It is somewhat surprising that not more work had been extended until recently to justify the viscous Moore-Greitzer equations, given all the work that has been put into analyzing and controlling their solutions. The jet engine flow is well described by the Navier-Stokes equations, but a full three-dimensional analysis of this equation is out of

reach of current technology. However, with more analysis one should be able to reduce the full Navier-Stokes equations and justify the use of the viscous Moore-Greitzer system. The main question is about the viscous term in the equations that was not included in the original equations by Moore and Greitzer. There were three questions about that term that people had puzzled over: Is is really there? Where did it come from? How big is it? In this paper we will answer these questions. It is there. It is caused by eddy viscosity and you can estimate its size. A lot of the mathematical analysis of the Moore-Greitzer equations in the literature is based on the fact that the PDE in Moore-Greitzer is a nonlinear parabolic equation. This is only the case is if the viscous term is there and cannot be ignored. The second question concerning the Moore-Greitzer equations was about the modeling of the forcing in the equations. It is modeled as a cubic equation in the flow velocity but the question remained whether gradient term should be included or not. We will show that because of the eddy viscosity small gradient terms should be included and we compute the correction.
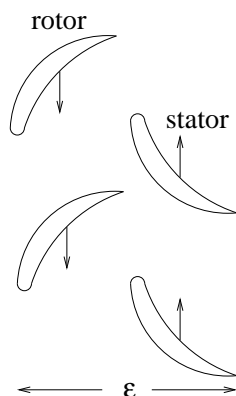

Figure 2: The local cell of rotor-stator pair as seen from the outside of the engine's casing, the arrows denote the movement of the blades viewed in the frame rotating with half the speed of the rotors.

The derivation of the Moore-Greitzer equation, see [30] and [23], is based on a quasi-steady flow approximation. The flow in the compressor is first assumed to be axisymmetric and in a steady state and then terms are added to represent the time dependent and non-axisymmetric flow effects. The flow instabilities surge and stall as well as non-uniformities in the inlet flow are relatively large length scale and long time scale flow phenomena compared to the length scale of the blade pitch and time scale of a blade passage (rotor-stator pair) convection, see [23]. Thus the conventional Moore-Greitzer model represent the effective performance of the blades when averaged over the short length and time scales. Although this approach undoubtedly yields the qualitatively correct results it is difficult to make mathematically rigorous. The main reason is that the flow through the compressor is not steady. On the contrary the flow is very turbulent on the scale of the blade passage, there are boundary layers, vortices peal of the ends of the blades and the interpassage flow can be extremely complicated.

In this paper we start with the Navier-Stokes equation and use stochastic homogenization theory of fluids, see also Hou [15], to derive a modified version of the viscous Moore-Greitzer equation (12.2). The homogenization is based on the small scale (ϵ) represented by the blade pitch or the length of a blade passage, consisting of a rotor-stator pair, the fast time scale is given by the convection velocity through a rotor-stator cell, see Figure 2. Our homogenization is not rigorous because it is not clearly understood yet how the noise gets introduced into the fluid from the boundary of the rotor and stator blades. For a recent approach to how noise can be introduced into turbulent flow see [10]. We will simply assume that the flow is turbulent and stochastic homogenization can be used to get an averaged flow.

Compressibility of air is important in aeroengines and cannot be ignored in the combustor and afterburners, see Section 13. Our starting point are the incompressible Navier-Stokes equations so we are ignoring compressibility of air in the compressor. This is the conventional approach, see [30, 31, 13], but can it be justified? The theoretical insight gained by our approach is that the built-up pressure in the compressor is mostly due to built-up in stagnation pressure. The blades in the compressor accelerate the air and this acceleration increases the quantity $\frac{1}{2}u^2 + p/\rho$, familiar from Bernoulli's theorem, where u is velocity of air, p the pressure and ρ the density. This is the stagnation pressure and it increases from stage to stage in the compressor. Thus we can assume that the density is constant at each stage and increases as a monotone function, at most, with the number of stages. There may be small corrections to our equations if $\rho(z)$ increases with distance z into the compressors but these corrections can be computed by first order perturbation theory.

The mathematical approach in this paper, is based on the fact that there is a clear separation of scales. The details of the flow on the scale determined by the blade pitch and cross-sectional length, and blade passage convection, are irrelevant for the large scale flow as long as the cumulative effect on the large scale flow is captured. This is precisely what the stochastic homogenization permits one to do. By separating the large and small scale flow and then averaging over the small scale in the large scale equations one gets the effective large scale flow. This then allows one to explain why the quasi-steady approximation, see [30] and [23], did give good results for the spatially largest Fourier components. It was because the approximation was good for the flow in these very largest scales.

Most importantly for the general theory, we give a generalized model (9.18) that can easily be solved numerically and analyzed. We do this by introducing three different time scales: the fast time scale which describes the turbulent flow in the unit (rotor-stator) cell; the normal time scale associated with the rotation time of the rotors; and the slow time scale describing the large scale dynamics of the compressor. The asymmetric flow patterns in the jet engine are expected to have length scales that are of the order of the compressor diameter, see [30]. Therefore these patterns will change on a time scale that is much longer than that associated with the change in flow through the rotor-stator cell in Figure 2. This is the slow-time and large spatial scale that Moore and Greitzer [30]

were concerned with and that they expressed the final equation in terms of. In particular the evolution of the flow instabilities surge and stall involves these *large spatial* and *slow temporal* scales.

We will explain below how the two-step procedure for the homogenization of fluids discussed above, produced the Moore-Greitzer equations. To recap, these steps are the derivation of two equations:

- *A local equation* for the small spatial scales and fast-time flow

- *A global equation* for the large spatial scales and slow-time flow, where the small and fast scales have been averaged over

In addition to these equations we will find the equations for the flow on a time-scale comparable to the rotation time. This is called the normal time flow and consists of vortex tubes analogous to Rayleigh-Bénard convection rolls but in the complicated geometry of moving rotors and stators.

In the end one obtains a solution of the Navier-Stokes equations in the form

$$u^\epsilon(x,t) = \epsilon^{1/2} u^0(x,y,t_f,t,t_s) + \epsilon^{3/2} u^1(x,y,t_f,t,t_s) + \cdots$$

where u^0 is determined by the local and global equations (and the normal time equations), y is the vector of local coordinates, t_f and t_s are the fast and the slow time respectively, and $\epsilon < 1$ is not small. This raises the question how good an approximation $\epsilon^{1/2} u^0$ is to the real solution. The answer depends on u^1 that can be computed by homogenizing to a higher order. However, in many problems where there are fast oscillations present on a small scale it turns out that the error averages to something very small or zero, even for ϵ close to one. This is our explanation of why the Moore-Greitzer equation is a good model for jet engine flow.

The outline of this paper is as follows: in Section 2, we start with the scaled Navier-Stokes equations in cylindrical coordinates. The equations are made dimensionless in Section 3. The two-scales asymptotic expansion is performed in Section 4 and global and local equations are obtained. At the end of Section 4 we compute the normal time swirl and vortex tubes aligned along the axis of the jet engine, as far as it can be done without the geometric details. In Section 5, we analyze the mean velocity field of the global equation. In Section 6, we eliminate the local derivatives from the mean velocity field equations. In Section 7, we rewrite the mean velocity field equation to get an expression of the eddy viscosity and forcing terms. The improved model for the large scale and slow-time modulation of the flow in the jet engine is then spelled out at the end of Section 7. This result assumes that stochastic homogenization can be applied to the flow. In Section 9 we average the equations over the normal time periodic rotation (swirl) of the cylindrical vortex tubes. This yields our *New Model* for jet engine flow. In Section 10, we split the u_z equation into the mean flow and the deviation from it in order to compare with the Moore-Greitzer equation. In Section 11, we introduce the dynamic equation

for the pressure rise in the plenum and apply similar asymptotic expansion as above to obtain equations of different orders. In Section 12, we gather the results obtained from previous sections and write down the modified actuator disk model and compare it with the original viscous Moore-Greitzer equation. Here the correct eddy viscosity terms are discussed and the second main theorem, explaining what kind of approximation the viscous Moore-Greitzer equations are, is stated and proved. In Section 13 we explain how our analysis can be combined with analysis of the combustion in the plenum and the afterburners to get a mathematical model describing the whole engine, combining the compressor and the combustion. In Section 14 we simulate the New Model with two different types of simplifying assumptions and compare the results with simulations of the viscous Moore-Greitzer equations. Section 15 contains our conclusions.

2 The Navier-Stokes Equation

In this paper we study the jet engine flow through the compressor. This flow is governed by the Navier-Stokes equations. Our ultimate goal is to show that under certain assumption the solution to the viscous Moore-Greitzer equation is the stochastically homogenized limit of the solution to the Navier-Stokes equation. On the way we will obtain a generalization of the viscous Moore-Greitzer equation that describes the stability of the desired flow in the whole compressor. We will also obtain averaged Navier-Stokes equations that are numerically tractable.

We start with the scaled Navier-Stoke equations in Cartesian coordinates in the inertial frame:

$$
\begin{cases}
\dfrac{\partial u^\epsilon}{\partial t} + (u^\epsilon \cdot \bigtriangledown)\, u^\epsilon - \epsilon^{3/2} \nu \bigtriangleup u^\epsilon = -\dfrac{1}{\rho} \bigtriangledown p_\epsilon \\[2mm]
\bigtriangledown \cdot u^\epsilon = 0 \\[2mm]
u^\epsilon \mid_{t=0} = u_0^\epsilon \\[2mm]
n \cdot \nabla u = 0, \ \text{ boundary condition in the inlet and outlet ducts} \\
\quad \text{and } \ u^\epsilon = -\beta(x_0 \sin(\beta t) - y_0 \cos(\beta t), x_0 \cos(\beta t) + y_0 \sin(\beta t), 0) \\
\quad \text{on the rotor blades and the hub, i.e. the fluid follows the blades,} \\
\text{no}-\text{slip}, \ u = 0, \ \text{ boundary condition on the casing and the stator blades.}
\end{cases}
$$
$$(2.1)$$

Here Ω_ϵ is the domain, u^ϵ is the velocity vector field, t is the normal time, p_ϵ is the pressure, ρ is the density and ν is the kinematic viscosity of the air. The superscript ϵ means that the variables depend on a parameter ϵ, which is the spatial period of the stator-rotor pair, see Figure 2. We note that the domain Ω_ϵ depends on ϵ since the solutions, u^ϵ, only exist in-between the blades and the casing and the hub, see Figure

2. When ϵ is decreasing it corresponds to increased number of blades and a decreased distance between the hub and the casing. See also Figure 1 for the domain of the above equation. We are assuming that the rotors and the hub rotate in a clockwise direction. The boundary conditions imply that the flow has no relative movement on the boundary. For example, if we are in the inertial frame, then $u^\epsilon=0$ on the casing as well as on the stators and u^ϵ is the same as the velocity of the rotors on the rotors and on the hub.

Due to the incompressibility $\rho =$ constant and we will take $\rho = 1$ below by a rescaling of the pressure. Strict incompressibility is not satisfied in jet engine compressors. However, it is likely that this will lead to quantitative rather than qualitative differences with the theory presented below. We present the results in this paper as the first step towards a fully compressible model for jet engine flow.

Assume initial conditions are given. Globally, we prescribe steady flow in the inlet and outlet duct, $u^\epsilon = -\beta(x_1 \sin(\beta t) - y_1 \cos(\beta t), x_1 \cos(\beta t) + y_1 \sin(\beta t), 0)$ on the hub and no-slip on the casing as boundary conditions. Locally, we prescribe no-slip on the stators and $u^\epsilon = -\beta(x_0 \sin(\beta t) - y_0 \cos(\beta t), x_0 \cos(\beta t) + y_0 \sin(\beta t), 0)$ on the rotors as boundary conditions. We can extend the flow smoothly into the blades while obeying the boundary condition. This problem is locally well-posed, see [19], and globally well-posed if the initial data and the forcing are small, see for example [33] or [9].

The choice of scaling here, together with the choice of power in the asymptotic expansion later, is the unique choice that makes every term in the Navier-Stokes equation reappear in the leading order equation, after the asymptotic expansion, so that the structure is preserved on the small scale. The derivation of this choice can be found in [9], it was originally suggested by J. L. Lions in [22]. In [9] it is also shown that a priori estimates work for this scaling, again verifying its correctness.

We now rewrite the above equation in cylindrical coordinates in a rotating frame with *half* the speed of the rotors as follows:

$$
\begin{cases}
\dfrac{\partial u_z^\epsilon}{\partial t} + u_r^\epsilon \dfrac{\partial u_z^\epsilon}{\partial r} + \dfrac{u_\theta^\epsilon}{r}\dfrac{\partial u_z^\epsilon}{\partial \theta} + u_z^\epsilon \dfrac{\partial u_z^\epsilon}{\partial z} - \epsilon^{3/2}\nu \triangle u_z^\epsilon = -\dfrac{\partial p_\epsilon}{\partial z}, \\[4mm]
\dfrac{\partial u_r^\epsilon}{\partial t} + u_r^\epsilon \dfrac{\partial u_r^\epsilon}{\partial r} + \dfrac{u_\theta^\epsilon}{r}\dfrac{\partial u_r^\epsilon}{\partial \theta} - \dfrac{(u_\theta^\epsilon)^2}{r} + u_z^\epsilon \dfrac{\partial u_r^\epsilon}{\partial z} - \epsilon^{3/2}\nu(\triangle u_r^\epsilon - \dfrac{u_r^\epsilon}{r^2} - \dfrac{2}{r^2}\dfrac{\partial u_\theta^\epsilon}{\partial \theta}) = \\[4mm]
\qquad\qquad\qquad\qquad -\dfrac{\partial p_\epsilon}{\partial r} + \dfrac{\beta^2}{4}r + \beta u_\theta^\epsilon, \\[4mm]
\dfrac{\partial u_\theta^\epsilon}{\partial t} + u_r^\epsilon \dfrac{\partial u_\theta^\epsilon}{\partial r} + \dfrac{u_\theta^\epsilon}{r}\dfrac{\partial u_\theta^\epsilon}{\partial \theta} + \dfrac{u_r^\epsilon u_\theta^\epsilon}{r} + u_z^\epsilon \dfrac{\partial u_\theta^\epsilon}{\partial z} - \epsilon^{3/2}\nu(\triangle u_\theta^\epsilon - \dfrac{u_\theta^\epsilon}{r^2} + \dfrac{2}{r^2}\dfrac{\partial u_r^\epsilon}{\partial \theta}) = \\[4mm]
\qquad\qquad\qquad\qquad -\dfrac{\partial p_\epsilon}{\partial \theta} - \beta u_r^\epsilon,
\end{cases}
\tag{2.2}
$$

where $\triangle = \frac{1}{r}\frac{\partial}{\partial r} + \frac{\partial^2}{\partial r^2} + \frac{1}{r^2}\frac{\partial^2}{\partial \theta^2} + \frac{\partial^2}{\partial z^2}$ is the Laplacian differential operator in cylindrical coordinates, $u_z^\epsilon, u_r^\epsilon, u_\theta^\epsilon$ are the 3 components of the velocity field of the flow in cylindrical

9

coordinates and β is the angular velocity of the rotors. Due to the rotating frame with half the speed of the rotors, the Coriolis acceleration terms βu_θ^ϵ, $-\beta u_r^\epsilon$ (written as a cross product in vector form in [26]) and the centrifugal acceleration term $\frac{\beta^2}{4}r$ appear.

3   The dimensionless system

In order to compare the size of the various terms in the above equations we next non-dimensionalize the problem. We define dimensionless variables, denoted by the superscript $\tilde{}$ as follows: $u_z^\epsilon = U\tilde{u}_z^\epsilon$, $u_r^\epsilon = U\tilde{u}_r^\epsilon$, $u_\theta^\epsilon = U\tilde{u}_\theta^\epsilon$, $r = R\tilde{r}$, $z = L\tilde{z}$, $p_\epsilon = Q\tilde{p}^\epsilon$, $t = \frac{1}{\beta}\tilde{t}$, where $U = R\beta$, $Q = U^2$, $R = \frac{r_1+r_2}{2}$, (r_1 and r_2 are the inner and outer radius of the compressor, see Figure 1), $L = z_1 - z_0$ (z_0 and z_1 are the z-coordinates of the beginning and the end of the compressor respectively). The notations here are the same as in [26] and [14].

Suppressing the superscripts we get the dimensionless Navier-Stokes system

$$
\left\{
\begin{aligned}
&\frac{\partial u_z^\epsilon}{\partial t} + u_r^\epsilon \frac{\partial u_z^\epsilon}{\partial r} + \frac{u_\theta^\epsilon}{r}\frac{\partial u_z^\epsilon}{\partial \theta} + \frac{R}{L}u_z^\epsilon\frac{\partial u_z^\epsilon}{\partial z} \\
&-\frac{\epsilon^{3/2}\nu}{\beta R^2}\left(\frac{1}{r}\frac{\partial u_z^\epsilon}{\partial r} + \frac{\partial^2 u_z^\epsilon}{\partial r^2} + \frac{1}{r^2}\frac{\partial^2 u_z^\epsilon}{\partial \theta^2}\right) - \frac{\epsilon^{3/2}\nu}{\beta L^2}\frac{\partial^2 u_z^\epsilon}{\partial z^2} = -\frac{R}{L}\frac{\partial p_\epsilon}{\partial z}, \\
\\
&\frac{\partial u_r^\epsilon}{\partial t} + u_r^\epsilon \frac{\partial u_r^\epsilon}{\partial r} + \frac{u_\theta^\epsilon}{r}\frac{\partial u_r^\epsilon}{\partial \theta} - \frac{1}{r}(u_\theta^\epsilon)^2 + \frac{R}{L}u_z^\epsilon\frac{\partial u_r^\epsilon}{\partial z} - \frac{\epsilon^{3/2}\nu}{\beta R^2}\left(\frac{1}{r}\frac{\partial u_r^\epsilon}{\partial r} + \frac{\partial^2 u_r^\epsilon}{\partial r^2}\right. \\
&\left.+\frac{1}{r^2}\frac{\partial^2 u_r^\epsilon}{\partial \theta^2} - \frac{u_r^\epsilon}{r^2} - \frac{2}{r^2}\frac{\partial u_\theta^\epsilon}{\partial \theta}\right) - \frac{\epsilon^{3/2}\nu}{\beta L^2}\frac{\partial^2 u_r^\epsilon}{\partial z^2} = -\frac{\partial p_\epsilon}{\partial r} + \frac{r}{4} + u_\theta^\epsilon, \\
\\
&\frac{\partial u_\theta^\epsilon}{\partial t} + u_r^\epsilon \frac{\partial u_\theta^\epsilon}{\partial r} + \frac{u_\theta^\epsilon}{r}\frac{\partial u_\theta^\epsilon}{\partial \theta} + \frac{u_r^\epsilon u_\theta^\epsilon}{r} + \frac{R}{L}u_z^\epsilon\frac{\partial u_\theta^\epsilon}{\partial z} - \frac{\epsilon^{3/2}\nu}{\beta R^2}\left(\frac{1}{r}\frac{\partial u_\theta^\epsilon}{\partial r}+\right. \\
&\left.\frac{\partial^2 u_\theta^\epsilon}{\partial r^2} + \frac{1}{r^2}\frac{\partial^2 u_\theta^\epsilon}{\partial \theta^2} + \frac{2}{r^2}\frac{\partial u_r^\epsilon}{\partial \theta} - \frac{u_\theta^\epsilon}{r^2}\right) - \frac{\epsilon^{3/2}\nu}{\beta L^2}\frac{\partial^2 u_\theta^\epsilon}{\partial z^2} = -\frac{1}{r}\frac{\partial p_\epsilon}{\partial \theta} - u_r^\epsilon,
\end{aligned}
\right.
\tag{3.1}
$$

where the coefficients are now unitless. We will use these equations below to obtain equations for various orders of the small parameter ϵ. We remind the reader that these equations are written from the vantage point of an observer who is rotating in the $-\theta$ (clockwise) direction with half the speed of the rotor blades. Thus both the rotors and the stators are moving in this reference frame with the same speed but in opposite directions, see Figure 2.

4   Two-scales asymptotic expansions

We will now apply stochastic homogenization to the equations (3.1). Define the local variables $\zeta = \frac{z}{\epsilon}, \alpha = \frac{r}{\epsilon}, \kappa = \frac{\theta}{\epsilon}$, the fast time $\tau_f = \frac{t}{\sqrt{\epsilon}}$ and the slow time $\tau_s = \sqrt{\epsilon}t$. We concentrate on a unit cell $(\zeta, \alpha, \kappa) \in (0,1) \times (\frac{1}{2}, \frac{3}{2}) \times (0,1)$ and apply periodic boundary condition on local variables. Also consider $\tau_f \in (0,1)$ and assume that this fast time is also periodic with period 1. The reason why we get the local cell $(\frac{1}{2}, \frac{3}{2})$ for the radial variable, instead of the standard local cell $(0,1)$ is that the inner and outer radius for the compressor approach the mean radius $R = \frac{r_1 + r_2}{2}$ [1], r_1 being the radius of the hub and r_2 that of the casing, as $\epsilon \to 0$, which is then rescaled to one. If $\tilde{r}_1, \tilde{r}_2$ are the rescaled inner and outer radii, then $\tilde{r}_2 - \tilde{r}_1 = \epsilon$ and $\frac{\tilde{r}_1 + \tilde{r}_2}{2} = 1$ for every $\epsilon > 0$, and on the unit cell $\tilde{r}_2 - \tilde{r}_1 = 1$ which implies that the unit cell is $(\frac{1}{2}, \frac{3}{2})$. Another way of saying this is that when $\epsilon = 1$ then we have an engine where the distance between the hub and the casing is the same as the mean radius R. The angular and axial directions are easily rescaled to give the unit cell.

Note that having three different time scales is crucial: the fast time scale describes the turbulent flow in the unit cell, the normal time scale describes the rotation of the rotors, and the slow time scale describes the overall large scale dynamics of the flow in the compressor. In hot wire experiments [21] these time-scales appear well separated. That is to say, the small and fast turbulent scales are well separated from design flow and independent of large variations in the design flow. This is the fundamental separation of scales in the problem. The modulational instabilities are presented by a few (one, two or three) modes well separated from the turbulence although their appearance increases significantly the turbulent activity. These instabilities are not so well separated from design flow that they serve to make unstable. However, one can still justify the separation of the slow and the normal time scales by viewing the instabilities as a slow modulation acting on the scale of the whole compressor. This is analogous to averaging in ODEs, see [34].

---

[1] We recall that the domain Ω_ϵ depends on ϵ, and so do the radii of the hub and casing, even if this is not spelled out in the notation. A more consistent but cumbersome notation would be r_1^ϵ and $\tilde{r}_1^\epsilon$.

We make the following asymptotic expansion:

$$
\begin{cases}
u_z^\epsilon(z,r,\theta,t) = \sqrt{\epsilon}\sum_{i=0}^{\infty} \epsilon^i u_z^i(z,\dfrac{z}{\epsilon},r,\dfrac{r}{\epsilon},\theta,\dfrac{\theta}{\epsilon},\sqrt{\epsilon}t,t,\dfrac{t}{\sqrt{\epsilon}}), \\[2ex]
u_r^\epsilon(z,r,\theta,t) = \sqrt{\epsilon}\sum_{i=0}^{\infty} \epsilon^i u_r^i(z,\dfrac{z}{\epsilon},r,\dfrac{r}{\epsilon},\theta,\dfrac{\theta}{\epsilon},\sqrt{\epsilon}t,t,\dfrac{t}{\sqrt{\epsilon}}), \\[2ex]
u_\theta^\epsilon(z,r,\theta,t) = \sqrt{\epsilon}\sum_{i=0}^{\infty} \epsilon^i u_\theta^i(z,\dfrac{z}{\epsilon},r,\dfrac{r}{\epsilon},\theta,\dfrac{\theta}{\epsilon},\sqrt{\epsilon}t,t,\dfrac{t}{\sqrt{\epsilon}}), \\[2ex]
p_\epsilon(z,r,\theta,t) = \sum_{i=0}^{\infty} \epsilon^i p_i(z,\dfrac{z}{\epsilon},r,\dfrac{r}{\epsilon},\theta,\dfrac{\theta}{\epsilon},\sqrt{\epsilon}t,t,\dfrac{t}{\sqrt{\epsilon}}),
\end{cases}
\tag{4.1}
$$

The scaling here is the same as in [9], except for the introduction of the slow time, $\sqrt{\epsilon}t$. As we mentioned before, this is the unique scaling that preserves the structure of the Navier-Stokes equation in the leading order equation. However this scaling does break the invariance of the Navier-Stokes equation. This must be done in problems that have separation of scales: what is happening on the small scale is independent of what is happening on the large scale. Thus the problem is not scale invariant.

Substituting these expansions into the non-dimensional Navier-Stokes equations (3.1) and applying the chain rule:

$$
\frac{\partial}{\partial z} = \frac{\partial}{\partial z} + \frac{1}{\epsilon}\frac{\partial}{\partial \zeta}, \quad \frac{\partial}{\partial r} = \frac{\partial}{\partial r} + \frac{1}{\epsilon}\frac{\partial}{\partial \alpha}, \quad \frac{\partial}{\partial \theta} = \frac{1}{r}\frac{\partial}{\partial \theta} + \frac{1}{r\epsilon}\frac{\partial}{\partial \kappa}, \quad \frac{\partial}{\partial t} = \sqrt{\epsilon}\frac{\partial}{\partial \tau_s} + \frac{\partial}{\partial t} + \frac{1}{\sqrt{\epsilon}}\frac{\partial}{\partial \tau_f},
$$

we obtain the following equations by gathering terms of the same order:

ϵ^{-1} terms:

$$
\begin{cases}
\dfrac{\partial p_0}{\partial \zeta} = 0, & z-\text{ equation}, \\[2ex]
\dfrac{\partial p_0}{\partial \alpha} = 0, & r-\text{ equation}, \\[2ex]
\dfrac{\partial p_0}{\partial \kappa} = 0, & \theta-\text{ equation}.
\end{cases}
\tag{4.2}
$$

This simply says that we have $\nabla_y p_0 = 0$, i.e. p_0 does not depend on the local scale, where the vector $y = (\zeta, \alpha, \kappa)$ denotes the local scale.

The ϵ^0 terms give us the local equation, containing the fast time scale, of the Navier-Stokes equation:

The Local Equations

$$
\begin{cases}
\begin{aligned}
&\frac{\partial u_z^0}{\partial \tau_f} + u_r^0 \frac{\partial u_z^0}{\partial \alpha} + \frac{1}{r} u_\theta^0 \frac{\partial u_z^0}{\partial \kappa} + \frac{R}{L} u_z^0 \frac{\partial u_z^0}{\partial \zeta} \\[2mm]
&-\frac{\nu}{\beta R^2} \left(\frac{\partial^2 u_z^0}{\partial \alpha^2} + \frac{1}{r^2} \frac{\partial^2 u_z^0}{\partial \kappa^2} \right) - \frac{\nu}{\beta L^2} \frac{\partial^2 u_z^0}{\partial \zeta^2} = -\frac{R}{L} \left(\frac{\partial p_0}{\partial z} + \frac{\partial p_1}{\partial \zeta} \right), \\[4mm]
&\frac{\partial u_r^0}{\partial \tau_f} + u_r^0 \frac{\partial u_r^0}{\partial \alpha} + \frac{1}{r} u_\theta^0 \frac{\partial u_r^0}{\partial \kappa} + \frac{R}{L} u_z^0 \frac{\partial u_r^0}{\partial \zeta} \\[2mm]
&-\frac{\nu}{\beta R^2} \left(\frac{\partial^2 u_r^0}{\partial \alpha^2} + \frac{1}{r^2} \frac{\partial^2 u_r^0}{\partial \kappa^2} \right) - \frac{\nu}{\beta L^2} \frac{\partial^2 u_r^0}{\partial \zeta^2} = -\left(\frac{\partial p_0}{\partial r} + \frac{\partial p_1}{\partial \alpha} \right) + \frac{r}{4}, \\[4mm]
&\frac{\partial u_\theta^0}{\partial \tau_f} + \left(u_r^0 \frac{\partial u_\theta^0}{\partial \alpha} + \frac{1}{r} u_\theta^0 \frac{\partial u_\theta^0}{\partial \kappa} \right) + \frac{R}{L} u_z^0 \frac{\partial u_\theta^0}{\partial \zeta} \\[2mm]
&-\frac{\nu}{\beta R^2} \left(\frac{\partial^2 u_\theta^0}{\partial \alpha^2} + \frac{1}{r^2} \frac{\partial^2 u_\theta^0}{\partial \kappa^2} \right) - \frac{\nu}{\beta L^2} \frac{\partial^2 u_\theta^0}{\partial \zeta^2} = -\frac{1}{r} \left(\frac{\partial p_0}{\partial \theta} + \frac{\partial p_1}{\partial \kappa} \right).
\end{aligned}
\end{cases}
\tag{4.3}
$$

This system describes the turbulent flow in the small scales. The boundary conditions for this system are $u = 0$ on the hub and the casing and on the blades, and $n \cdot \nabla u = 0$ in the inlet and the outlet ducts. The blades are stationary in the local equations but the velocity is extended to be constant inside the blades. We clearly need to know the detailed geometry of the blades to get an exact solution. However, since we have separation of scales in the jet engine flow, what is happening in the large scales is independent of these details as long as the cumulative effect, appearing later as eddy viscosity, on the large scales is captured. This will prompt us to average over the local scales in the next section.

The $\epsilon^{1/2}$ terms give us the normal time information in the Navier-Stokes equation:

$$
\begin{cases}
\dfrac{\partial u_z^0}{\partial t} = 0, \\[4mm]
\dfrac{\partial u_r^0}{\partial t} = u_\theta^0, \\[4mm]
\dfrac{\partial u_\theta^0}{\partial t} = -u_r^0 .
\end{cases}
\tag{4.4}
$$

This normal time flow takes place in the geometry of moving rotors and stators, with the flow velocity being equal to the velocity of the rotors and the stators at the boundary. The boundary conditions on the hub become

$$
u_\theta = \frac{1}{2}, \ u_r = 0 = u_z,
$$

13

and at the casing

$$u_\theta = -\frac{1}{2}, \ u_r = 0 = u_z.$$

These are the velocities of the hub and the casing with respect to an observer moving at half the velocity of the rotors.
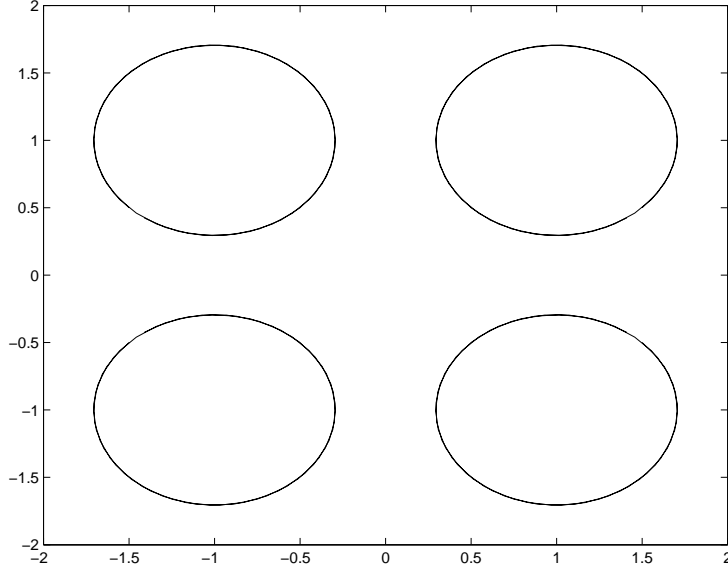

Figure 3: The normal time periodic rotation cells in the annulus between the hub and the casings.

The normal time equations describe the flow due to the Coriolis force stemming from the acceleration. The equations are most easily solved in Cartesian coordinates where they give clockwise rotation of the flow about some center with angular velocity 1. In Cartesian coordinates the normal time equations become

$$
\begin{cases}
\dfrac{\partial u_z^0}{\partial t} = 0, \\[2ex]
\dfrac{\partial u_x^0}{\partial t} = u_y^0, \\[2ex]
\dfrac{\partial u_y^0}{\partial t} = -u_x^0 \ ,
\end{cases}
\tag{4.5}
$$

and are easily solved. The Cartesian velocity vectors have the form : $u_x^0 = a\cos(t) + b\sin(t), u_y^0 = -a\sin(t) + b\cos(t), u_z = c$. If the coefficients a, b and c are constant, these

equations are easily solved for the streamlines

$$
\begin{array}{rcl}
x(t) = r\cos(\theta) + x_0 & = & (a\sin(t) - b\cos(t)) + x_0 \\
y(t) = r\sin(\theta) + y_0 & = & (a\cos(t) + b\sin(t)) + y_0 \\
z(t) & = & z_0 + ct,
\end{array}
\tag{4.6}
$$

These streamlines are analogous to the flow lines of cylindrical Rayleigh-Bénard convection rolls in Rayleigh-Bénard flow, see [20], but with constant flow in the z direction. The simplest solution is a circular flow $(x_0, y_0) = (0, 0)$ and $r > 1/2$ around the hub that modifies the normal time flow rotation. This solution is responsible for fluctuation in the normal time swirling flow. The rest of the solutions consist of vortex tubes of periodic (in the radial and angular components of the velocity) flow in the annulus between the hub and casing, see Figure 3. These solutions can be expected to play a role in the instabilities of the swirling flow. The period of the flow is 2π as stipulated by normalized angular velocity $\beta = 1$. However, in order to satisfy the boundary conditions in a realistic geometry, the coefficients a, b and c are functions of the variables x, y and z in addition to the local variables and fast and slow times and then the streamlines become more complex. The general form is an axial vortex tube similar to flow spiraling around a Rayleigh-Bénard rotation roll. The difference between the Rayleigh-Bénard convection rolls and ours is that the Rayleigh-Bénard rolls alternate their direction of rotation but our rolls all rotate in the same clockwise direction along the clockwise direction of the rotors and the hub. In fact they do satisfy the boundary conditions on the hub and the casing, instead on the hub their velocity is

$$
u_\theta = \frac{1}{2}, \ u_r = 0 = u_z,
$$

whereas at the casing

$$
u_\theta = -\frac{1}{2}, \ u_r = 0 = u_z.
$$

This means that the rolls inside the annulus, see Figure 3, are unstable.

Notice that when $t = 2n\pi$, we get $u_x^0 = a$ and $u_y^0 = b$. The Poincaré map of the normal time is defined to be value of u at times $t = nT$ where T determines a fixed normal time interval. Since we take very small time steps in the slow time τ_s for every time step of size T in normal time, we can consider the average over the local scale and fast time, where these averages are a good approximation to the (normal-time) Poincaré map of u. This is the point of view in the remainder of the paper. In other words by averaging out the fast motion and local scales and considering the slow and large-scale modulation of the normal time periodic motion, given above, we get a good flow approximation to the normal-time Poincaré map. This is analogous to the averaging method for ODEs, see for example [34].

The Global Equations

The ϵ^1 terms give us the global slow time Navier-Stokes equation. These equations fill a whole page and have been placed in the Appendix A. The system of equations describes the velocity field in the large scales. In the following sections, we will derive the Moore-Greitzer equation from this system.

5   The mean velocity field

The next step in the standard homogenization procedure is to average out the local variables from the global equation while applying the periodic boundary condition. The goal of this step is to average out what is happening in the small scales and see what the large scale outcome is, including the cumulative influence of the small scales.

Taking the average over the local variables ζ, α, κ and fast time τ_f in (A.9) and using the periodicity in the local spacial variables and fast time yields:

$$
\begin{cases}
\dfrac{\partial \overline{u_z^0}}{\partial \tau_s} + \overline{u_r^0 \dfrac{\partial u_z^0}{\partial r}} + \overline{u_r^0 \dfrac{\partial u_z^1}{\partial \alpha}} + \overline{u_r^1 \dfrac{\partial u_z^0}{\partial \alpha}} \; + \dfrac{1}{r}\left(\overline{u_\theta^0 \dfrac{\partial u_z^0}{\partial \theta}} + \overline{u_\theta^0 \dfrac{\partial u_z^1}{\partial \kappa}} + \overline{u_\theta^1 \dfrac{\partial u_z^0}{\partial \kappa}} \right) \\[4mm]
\qquad\qquad\qquad + \dfrac{R}{L}\overline{u_z^0 \dfrac{\partial u_z^0}{\partial z}} \; = -\dfrac{R}{L}\dfrac{\partial \overline{p_1}}{\partial z}, \\[4mm]
\dfrac{\partial \overline{u_r^0}}{\partial \tau_s} + \overline{u_r^0 \dfrac{\partial u_r^0}{\partial r}} + \dfrac{1}{r}\left(\overline{u_\theta^0 \dfrac{\partial u_r^0}{\partial \theta}} + \overline{u_\theta^0 \dfrac{\partial u_r^1}{\partial \kappa}} + \overline{u_\theta^1 \dfrac{\partial u_r^0}{\partial \kappa}} \right) \\[4mm]
+ \dfrac{R}{L}\left(\overline{u_z^0 \dfrac{\partial u_r^0}{\partial z}} + \overline{u_z^0 \dfrac{\partial u_r^1}{\partial \zeta}} + \overline{u_z^1 \dfrac{\partial u_r^0}{\partial \zeta}} \right) - \dfrac{1}{r}\overline{(u_\theta^0)^2} = -\dfrac{\partial \overline{p_1}}{\partial r}, \\[4mm]
\dfrac{\partial \overline{u_\theta^0}}{\partial \tau_s} + \overline{u_r^0 \dfrac{\partial u_\theta^0}{\partial r}} + \overline{u_r^0 \dfrac{\partial u_\theta^1}{\partial \alpha}} + \overline{u_r^1 \dfrac{\partial u_\theta^0}{\partial \alpha}} + \dfrac{1}{r}\overline{u_\theta^0 \dfrac{\partial u_\theta^0}{\partial \theta}} + \dfrac{1}{r}\overline{u_r^0 u_\theta^0} \\[4mm]
\qquad\qquad + \dfrac{R}{L}\left(\overline{u_z^0 \dfrac{\partial u_\theta^0}{\partial z}} + \overline{u_z^0 \dfrac{\partial u_\theta^1}{\partial \zeta}} + \overline{u_z^1 \dfrac{\partial u_\theta^0}{\partial \zeta}} \right) = -\dfrac{1}{r}\dfrac{\partial \overline{p_1}}{\partial \theta},
\end{cases}
\tag{5.1}
$$

where

$$
\overline{u_z^0}(z, r, \theta, \tau_s, t) = \int_0^1 \int_{\frac{1}{2}}^{\frac{3}{2}} \int_0^1 \int_0^1 u_z^0 \, d\zeta \, d\kappa \, d\alpha \, d\tau_f
$$

denotes the average over the local variables and fast time, and similarly for the other components. The equations are much simpler than the global equations in Appendix A, due to the cancellations that take place. The interior boundary (the blades) in the fluid are removed by the averaging but we are left with vanish boundary condition on the hub and the casing and $n \cdot \nabla u = 0$ in the inlet and outlet ducts.

6 The derivatives of the local variable eliminated

The mean velocity field equations contain both global and local variable derivatives. We want to eliminate the local variable derivatives by using incompressability and integration by parts. This dramatically simplifies our equations.

The non-dimensionalized continuity equation in cylindrical coordinates is:

$$\frac{\partial u_r^\epsilon}{\partial r} + \frac{1}{r}\frac{\partial u_\theta^\epsilon}{\partial \theta} + \frac{R}{L}\frac{\partial u_z^\epsilon}{\partial z} + \frac{u_r^\epsilon}{r} = 0 \tag{6.1}$$

The coefficient $\frac{R}{L}$ is introduced by the non-dimensionalization procedure in Section 3.

We perform the same two-scale asymptotic expansion as before and get the following equations:

$\epsilon^{-1/2}$ equation:

$$\frac{\partial u_r^0}{\partial \alpha} + \frac{1}{r}\frac{\partial u_\theta^0}{\partial \kappa} + \frac{R}{L}\frac{\partial u_z^0}{\partial \zeta} = 0 \tag{6.2}$$

$\epsilon^{1/2}$ equation:

$$\frac{\partial u_r^0}{\partial r} + \frac{1}{r}\frac{\partial u_\theta^0}{\partial \theta} + \frac{R}{L}\frac{\partial u_z^0}{\partial z} + \frac{u_r^0}{r} + \frac{\partial u_r^1}{\partial \alpha} + \frac{1}{r}\frac{\partial u_\theta^1}{\partial \kappa} + \frac{R}{L}\frac{\partial u_z^1}{\partial \zeta} = 0 \tag{6.3}$$

We substitute in these two equations and integrate by parts in the mean velocity field equations (5.1) to eliminate the local variable derivatives and reduce (5.1) to:

$$\begin{cases} \dfrac{\partial \overline{u_z^0}}{\partial \tau_s} + \dfrac{1}{r}\dfrac{\partial}{\partial r}\left(r\overline{u_r^0 u_z^0}\right) + \dfrac{1}{r}\dfrac{\partial}{\partial \theta}\left(\overline{u_\theta^0 u_z^0}\right) + \dfrac{R}{L}\dfrac{\partial}{\partial z}\overline{(u_z^0)^2} = -\dfrac{R}{L}\dfrac{\partial \overline{p_1}}{\partial z}, \\[3ex] \dfrac{\partial \overline{u_r^0}}{\partial \tau_s} + \dfrac{1}{r}\dfrac{\partial}{\partial r}\left(r\overline{(u_r^0)^2}\right) + \dfrac{1}{r}\dfrac{\partial}{\partial \theta}\left(\overline{u_r^0 u_\theta^0}\right) + \dfrac{R}{L}\dfrac{\partial}{\partial z}\left(\overline{u_r^0 u_z^0}\right) - \dfrac{1}{r}\overline{(u_\theta^0)^2} = -\dfrac{\partial \overline{p_1}}{\partial r}, \\[3ex] \dfrac{\partial \overline{u_\theta^0}}{\partial \tau_s} + \dfrac{1}{r^2}\dfrac{\partial}{\partial r}\left(r^2\overline{u_\theta^0 u_r^0}\right) + \dfrac{1}{r}\dfrac{\partial}{\partial \theta}\overline{(u_\theta^0)^2} + \dfrac{R}{L}\dfrac{\partial}{\partial z}\left(\overline{u_\theta^0 u_z^0}\right) + \dfrac{1}{r}\overline{u_r^0 u_\theta^0} = -\dfrac{1}{r}\dfrac{\partial \overline{p_1}}{\partial \theta}. \end{cases} \tag{6.4}$$

The large global equations in the Section 4 consuming one page in Appendix A are now reduced to three lines after averaging over the local scales and elimination by incompressability.

7 Eddy viscosity, forcing and the new model

The u_z equation in (6.4) must now be rewritten to compare with the Moore-Greitzer equation (1.1). Recall that in the Moore-Greitzer equation, we have an eddy viscosity term [18] which is the second derivative of θ, a transport term which is the first derivative

of θ, and a forcing term which is modeled by a cubic polynomial. Since we use a rotating frame with half the speed of the rotor and the original Moore-Greitzer equation is in the inertial frame, we will not have the transport term as in the Moore-Greitzer equation. Our goal is to rewrite the u_z equation to explicitly express the eddy viscosity term and the forcing term as follows:

$$\frac{\partial \overline{u_z^0}}{\partial \tau_s} = \nabla \cdot \left(A \nabla \overline{u_z^0} \right) + F_z \tag{7.1}$$

where A is a 3 by 3 eddy viscosity matrix coefficient and F_z is the forcing term. We are going to find formulas for A and F_z.

Firstly, we rewrite the eddy viscosity term in the component form as follows:

$$\nabla \cdot \left(A \nabla \overline{u_z^0} \right) = \frac{\partial}{\partial z}\left(a_{11}\frac{\partial \overline{u_z^0}}{\partial z} \right) + \frac{1}{r}\frac{\partial}{\partial z}\left(a_{12}\frac{\partial \overline{u_z^0}}{\partial \theta} \right) + \frac{\partial}{\partial z}\left(a_{13}\frac{\partial \overline{u_z^0}}{\partial r} \right)$$

$$+ \frac{1}{r}\frac{\partial}{\partial \theta}\left(a_{21}\frac{\partial \overline{u_z^0}}{\partial z} \right) + \frac{1}{r^2}\frac{\partial}{\partial \theta}\left(a_{22}\frac{\partial \overline{u_z^0}}{\partial \theta} \right) + \frac{1}{r}\frac{\partial}{\partial \theta}\left(a_{23}\frac{\partial \overline{u_z^0}}{\partial r} \right) \tag{7.2}$$

$$+ \frac{\partial}{\partial r}\left(a_{31}\frac{\partial \overline{u_z^0}}{\partial z} \right) + \frac{1}{r}\frac{\partial}{\partial r}\left(a_{32}\frac{\partial \overline{u_z^0}}{\partial \theta} \right) + \frac{\partial}{\partial r}\left(a_{33}\frac{\partial \overline{u_z^0}}{\partial r} \right) + \frac{1}{r}a_{31}\frac{\partial \overline{u_z^0}}{\partial z} + \frac{1}{r}a_{33}\frac{\partial \overline{u_z^0}}{\partial r},$$

where the coefficients a_{ij} are listed in Appendix B. Due to the cylindrical coordinates there are some first derivative terms present.

We will now look for solutions with the deviation of the velocity from the mean an inner product of the gradient of global variables with a vector depending on the local variables and fast time only:

$$\begin{cases} u_z^0 = \overline{u_z^0} + \nabla \overline{u_z^0} \cdot \chi^z\left(\zeta, \kappa, \alpha, \tau_f \right) \\[2mm] u_r^0 = \overline{u_r^0} + \nabla \overline{u_r^0} \cdot \chi^r\left(\zeta, \kappa, \alpha, \tau_f \right) \\[2mm] u_\theta^0 = \overline{u_\theta^0} + \nabla \overline{u_\theta^0} \cdot \chi^\theta\left(\zeta, \kappa, \alpha, \tau_f \right). \end{cases} \tag{7.3}$$

Note that $\overline{\chi^z} = \overline{\chi^r} = \overline{\chi^\theta} = 0$.

The equations for the components of the eddy viscosity tensor χ are obtained by substituting (7.3) into the local equation (4.3). This is called the cell problem,

$$\frac{\partial \chi}{\partial \tau_f} = \Delta_y \chi, \tag{7.4}$$

with periodic boundary conditions on the local cell. It is accompanied by a nonlinear version of Darcy's Law

$$(\overline{u^0} + \chi^z\,(y,\tau_f)\cdot\nabla_x\overline{u^0})\nabla_y\chi^z\,(y,\tau_f)\,\nabla_x\overline{u^0} = -(\nabla_x p_0 + \nabla_y p_1),\qquad(7.5)$$

determining the pressure gradient $\nabla_y p_1$ up to terms coming from the boundary.

We now write each term in the u equation of (6.4) in terms of $\overline{u^0_z}$, $\overline{u^0_\theta}$, $\overline{u^0_r}$, χ^z, χ^θ and χ^r, denoting the 3 components of χ^z as χ^z_z, χ^z_θ and χ^z_r and similarly for χ^θ and χ^r, and then compare the coefficient of each derivative term with the matrix coefficient. After some calculation we write down the equations and the forcing terms as follows. The coefficients of the eddy viscosity matrices A, B and C are placed in the appendix B.

The z equations is:

$$\frac{\partial\overline{u^0_z}}{\partial\tau_s} = \bigtriangledown\cdot\left(A\bigtriangledown\overline{u^0_z}\right) + F_z,\qquad(7.6)$$

where

$$F_z = -\frac{R}{L}\overline{u^0_z}\frac{\partial\overline{u^0_z}}{\partial z} - \frac{1}{r}\overline{u^0_\theta}\frac{\partial\overline{u^0_z}}{\partial\theta} - \overline{u^0_r}\frac{\partial\overline{u^0_z}}{\partial r} - \frac{R}{L}\frac{\partial\overline{p_1}}{\partial z}.\qquad(7.7)$$

Similarly, we rewrite the r equation as follows:

$$\frac{\partial\overline{u^0_r}}{\partial\tau_s} = \bigtriangledown\cdot\left(B\bigtriangledown\overline{u^0_r}\right) + F_r,\qquad(7.8)$$

where

$$F_r = -\frac{R}{L}\overline{u^0_z}\frac{\partial\overline{u^0_r}}{\partial z} - \frac{1}{r}\overline{u^0_\theta}\frac{\partial\overline{u^0_r}}{\partial\theta} - \overline{u^0_r}\frac{\partial\overline{u^0_r}}{\partial r} + \frac{1}{r}\overline{u^0_\theta}^2 - \frac{\partial\overline{p_1}}{\partial r} + \frac{1}{r}\overline{\nabla u^0_\theta}\cdot\overline{\chi^\theta\otimes\chi^\theta}\cdot\nabla\overline{u^0_\theta}.\qquad(7.9)$$

Also for θ equation, we rewrite it as:

$$\frac{\partial\overline{u^0_\theta}}{\partial\tau_s} = \bigtriangledown\cdot\left(C\bigtriangledown\overline{u^0_\theta}\right) + F_\theta,\qquad(7.10)$$

where

$$F_\theta = -\frac{R}{L}\overline{u^0_z}\frac{\partial\overline{u^0_\theta}}{\partial z} - \frac{1}{r}\overline{u^0_\theta}\frac{\partial\overline{u^0_\theta}}{\partial\theta} - \overline{u^0_r}\frac{\partial\overline{u^0_\theta}}{\partial r} - \frac{1}{r}\overline{u^0_r u^0_\theta} - \frac{1}{r}\overline{\nabla u^0_r}\cdot\overline{\chi^r\otimes\chi^\theta}\cdot\nabla\overline{u^0_\theta} - \frac{1}{r}\frac{\partial\overline{p_1}}{\partial\theta}.\qquad(7.11)$$

The three global averaged equations with eddy viscosity can now be written as

$$\begin{cases} \dfrac{\partial\overline{u}}{\partial\tau_s} + \overline{u}\cdot\nabla\overline{u} - \nabla\cdot(\mathcal{A}\nabla\,\overline{u}) = -\nabla\overline{p_1} + g \\[2ex] \nabla\cdot\overline{u} = 0 \end{cases}\qquad(7.12)$$

where $\mathcal{A}$ is the eddy viscosity tensor, $\mathcal{A}\nabla\overline{u}$ denotes the 3×3 matrix $(A\nabla\overline{u^0_z}, B\nabla\overline{u^0_r}, C\nabla\overline{u^0_\theta})$, and we have split the force $F = (F_z, F_r, F_\theta)$ into inertial terms and the pressure gradient

$\nabla \overline{p_1} = (\frac{\partial \overline{p_1}}{\partial z}, \frac{\partial \overline{p_1}}{\partial r}, \frac{1}{r}\frac{\partial \overline{p_1}}{\partial \theta})$, where all the z derivative are interpreted to be $\frac{R}{L}\frac{\partial}{\partial z}$. In addition there is a term $g = (0, (\frac{1}{r})\overline{u_\theta^0}^2 + (\frac{1}{r})\overline{\nabla u_\theta^0 \cdot \chi^\theta \otimes \chi^\theta \cdot \nabla u_\theta^0}, -\frac{1}{r}\overline{u_r^0 u_\theta^0} - \frac{1}{r}\overline{\nabla u_r^0 \cdot \chi^r \otimes \chi^\theta \cdot \nabla u_\theta^0})$ due to the Coriolis forces and the cylindrical coordinates and the associated viscosity. Notice that the local geometry (rotors and stators) has been averaged out so there is no longer an internal boundary in the fluid.

The equation (7.12) can be solved numerically on a *coarse grid*. However, we still need an equation for the pressure p_1.

The pressure equation is derived by taking divergence on both sides of the Navier-Stokes equations and performing the same asymptotic expansion as before. The details are similar to the derivation in Section 4 and therefore omitted. We obtain the following Poisson equation for p_1.

$$\triangle_y p_1 = \frac{8}{r}\csc^2(2\theta)\left(\frac{\partial u_r^0}{\partial \alpha}\frac{\partial u_\theta^0}{\partial \kappa} - \frac{\partial u_\theta^0}{\partial \alpha}\frac{\partial u_r^0}{\partial \kappa}\right) + 4\frac{L}{R}\left(\frac{\partial u_r^0}{\partial \alpha}\frac{\partial u_z^0}{\partial \zeta} - \frac{\partial u_z^0}{\partial \alpha}\frac{\partial u_r^0}{\partial \zeta}\right)$$

$$+\frac{4}{r}\frac{L}{R}\left(\frac{\partial u_\theta^0}{\partial \kappa}\frac{\partial u_z^0}{\partial \zeta} - \frac{\partial u_z^0}{\partial \kappa}\frac{\partial u_\theta^0}{\partial \zeta}\right) + 4\cot(2\theta)\frac{L}{R}\left(\frac{\partial u_\theta^0}{\partial \alpha}\frac{\partial u_z^0}{\partial \zeta} - \frac{\partial u_z^0}{\partial \alpha}\frac{\partial u_\theta^0}{\partial \zeta}\right) \qquad (7.13)$$

$$+\frac{4}{r}\cot(2\theta)\frac{L}{R}\left(\frac{\partial u_z^0}{\partial \kappa}\frac{\partial u_r^0}{\partial \zeta} - \frac{\partial u_r^0}{\partial \kappa}\frac{\partial u_z^0}{\partial \zeta}\right)$$

where $\triangle_y$ is the scaled Laplacian operator for the local variables, i.e., there is a coefficient $\frac{L}{R}$ in front of the ζ derivative. The scaling is the same as in Section 3.

Detailed local geometry is required to solve this equation for all the local cells. We refer to Figure 2 for the geometry and the boundary condition of the local cells. The boundary conditions on the pressure are that $\nabla p = 0$ in the inlet and outlet of the cell, see Figure 2, and ∇p is given on the rotor and stator blades. The solution becomes

$$p_1 = \int_Y G(z,y)f(z)dz - \int_{blades} G(z,y)\nabla p(z) \cdot n d\sigma(z), \qquad (7.14)$$

where f denotes the right hand side of the Poisson equation (7.13), G is the Green's function for the local cell $Y = T^3$, p is the boundary pressure on the blades and σ denotes the surface measure on the blades. The pressure gradient on the blades is simply the acceleration (divided by density $= 1$) that the fluid experiences as it enters the local cell. Averaging over the local scale we get

$$\overline{p_1}(x) = -\int_{blades} \overline{G^x(z,y)}\nabla p(z) \cdot n d\sigma(z), \qquad (7.15)$$

because $\overline{f} = 0$ by the equation (7.13) and G^x depends on x only through the local geometry. Notice that consistently the local average over the left hand side of (7.5) is

also zero. Thus the average of the pressure $\overline{p}_1$ is solely determined by the forcing by the blades.

The Improved Model

The two equations (7.12) and (7.15) give the numerically solvable model for the jet engine flow. The point is that $G^x(z, y)$ can be found numerically once the local geometry is known and then we can solve (7.16) on a coarse grid because all the fine structure in the flow has been averaged out. This computation can be performed with current computer technology.

Model 1:

The solution $\overline{u}$ of the improved model for jet engine flow

$$
\begin{cases}
\dfrac{\partial \overline{u}}{\partial \tau_s} + \overline{u} \cdot \nabla \overline{u} - \nabla \cdot (\mathcal{A} \nabla\, \overline{u}) = -\nabla \overline{p_1} + g(\overline{u}, \nabla \overline{u}) \\[2mm]
\overline{u}\mid_{t=0} = \overline{u}_0 \\[2mm]
\nabla \cdot \overline{u} = 0, \\[2mm]
n \cdot \nabla \overline{u} = 0, \text{ in the inlet and the outlet ducts} \\[2mm]
\text{and } \overline{u} = 0, \text{ on the hub and casing,}
\end{cases}
\tag{7.16}
$$

is the formal limit as $\epsilon \to 0$, of the solution to the Navier-Stokes equations (2.1), averaged (stochastically homogenized) over the local coordinates y and fast time t_f.

Recall that when the equations are written in polar coordinates then

$$
g = (0, \frac{1}{r}\overline{u_\theta^0}^2 + \frac{1}{r}\nabla \overline{u_\theta^0} \cdot \overline{\chi^\theta \otimes \chi^\theta} \cdot \nabla \overline{u_\theta^0}, \ -\frac{1}{r}\overline{u_r^0 u_\theta^0} - \frac{1}{r}\nabla \overline{u_r^0} \cdot \overline{\chi^r \otimes \chi^\theta} \cdot \nabla \overline{u_\theta^0}).
$$

$\mathcal{A}$ is the eddy viscosity tensor whose coordinates are given in Appendix B.

Remark 7.1 Model 1 is our assumption and we state it as a stochastically homogenized average. However, the average could also be taken to be a Reynolds Averaged Navier-Stokes (RANS) or Large Eddy Simulation (LES) model where a subgrid model is used to finds $\mathcal{A}$. Thus Model 1 can be interpreted to be a RANS or LES model and this taken as a starting point instead of a stochastic homogenization.

8   The Stochastic Homogenization

We will now recap briefly how the equations of the different order fit together in the stochastic homogenization theory. The ϵ of order -1 equation (4.2) give the independence of the global pressure p_0 of the local variable y. The ϵ of order 0 equation (4.3) is the Local Equation, it is nonlinear and cannot be solved explicitly but we can show that solutions exist. Its solvability condition

$$\nabla_x \overline{p_0} = -(p_1^{out} - p_1^{in}) + f_{cent},$$

where $f_{cent} = (0, r/4, 0)$, implies that the global pressure gradient balances the local pressure increase over the local cell. The ϵ of order $1/2$ equation (4.4) can be solved explicitly and produces the axial vortex tubes. Its solvability condition is trivial. The ϵ of order 1 equation (A.9) is in Appendix A. Its solvability condition is the Global Equation (6.4). That equation reduces to the Improved Model (7.16) after the introduction of the eddy viscosity tensor. Finally components of the eddy viscosity tensor satisfy the heat equation (7.4) with positive boundary data.

9   The average over normal time

The averaging over the normal-time periodic motion in Section 4 effects a tremendous simplification of the global equations describing the slow-time jet engine flow. This averaging amounts to an approximation of the Poincaré map associated with the periodic normal-time flow and is analogous to the averaging method for ODEs, see [34]. It is simplest to carry this averaging out in Cartesian coordinates so now we express the equations (7.1)-(7.10) is Cartesian coordinates.

We recall from Section 4 that the u_x^0 and the u_y^0 components of the (normal time) velocity (in the rotation frame) can be written in the form $u_x^0 = a\cos(t) + b\sin(t)$ and $u_y^0 = -a\sin(t) + b\cos(t)$, whereas u_z^0 does not depend on the normal time. We multiply the u_x^0 and u_y^0 equations (considered to be a two-vector) on the right by,

$$\begin{pmatrix} \cos(t) & \sin(t) \\ -\sin(t) & \cos(t) \end{pmatrix}$$

and average the three velocity equations (7.1)-(7.10) over the normal time period π. Recall that we have defined the derivative with respect to z to mean $\frac{R}{L}\frac{\partial}{\partial z}$.

This give the equations for the three velocity components in Theorem 9.1 and amounts to finding a slow modulation of the normal-time periodic orbit.

The New Model

Let the normal-time cylindrical rotation be

$$
\left(\begin{array}{c} \overline{u}_x^0 \\ \overline{u}_y^0 \end{array} \right) = \left(\begin{array}{cc} \cos(t) & \sin(t) \\ -\sin(t) & \cos(t) \end{array} \right) \left(\begin{array}{c} \overline{a} \\ \overline{b} \end{array} \right),
\tag{9.17}
$$

where $\overline{a}$ and $\overline{b}$ are still functions of the global variables and slow time.

Theorem 9.1 *The time average, of the $\overline{u}_z^0$ flow along the axis and the amplitude of the normal-time cylindrical rotation in the jet engine, is determined by the slow-time equations*

$$
\begin{cases}
\dfrac{\partial \overline{u_z^0}}{\partial \tau_s} + \overline{u_z^0} \dfrac{\partial \overline{u_z^0}}{\partial z} + \dfrac{\partial}{\partial z}(\nabla \overline{u_z^0} \cdot \overline{\chi^z \otimes \chi^z} \cdot \nabla \overline{u_z^0}) = -\dfrac{\partial \overline{p}_1}{\partial z} \\[3mm]
\dfrac{\partial \overline{a}}{\partial \tau_s} + \dfrac{\partial (\overline{u_z^0} \overline{a})}{\partial z} + \dfrac{\partial}{\partial z}\left(\overline{\chi^z a} \cdot \nabla \overline{u_z^0} \right) = 0 \\[3mm]
\dfrac{\partial \overline{b}}{\partial \tau_s} + \dfrac{\partial (\overline{u_z^0}\, \overline{b})}{\partial z} + \dfrac{\partial}{\partial z}\left(\overline{\chi^z b} \cdot \nabla \overline{u_z^0} \right) = 0.
\end{cases}
\tag{9.18}
$$

Their solutions are the averaged formal limit $\lim_{\epsilon \to 0} \epsilon^{-1/2} u^\epsilon$ of the solutions to the Navier-Stokes equations (2.1), averaged once more over the period of the rotation of the normal time vortex tubes (4.6).

Proof: The proof follows immediately from Model 1, using the normal-time averaging computation in this section. **QED**

The equations (9.18) determine the slow modulations of the cylindrical rotation rolls that are aligned with the (z) axis of the jet engine. They give more information than the Moore-Greitzer equations (1.1) but are much simpler to analyze than the improved model (7.1)-(7.10).

Remark 9.1 Notice that the flow in the z-direction $(\overline{u_z^0})$ is a slow addition to the constant normal time flow (design flow) in Section 4, whereas the flow in the r and θ directions is normal-time rotation with a slow modulation, given by the $\overline{a}$ and $\overline{b}$ equations above. It must be kept in mind, although we have not proven this, that we are in (9.18) approximating a Poincaré map by a flow and maps are different from a flow. However, this approximation gives the correct information about the map, see [34], including the stability of the solutions and their bifurcations.

We are actually done at this point. We have succeeded in deriving a model (9.18) for the jet engine flow that promises to be significantly better that the Moore-Greitzer equation. (Assuming of course that it tests well against experimental data.) Not only

does it have an equation (for $\overline{u}_z^0$) describing the flow in the z directions, this new model also contains two more equations (for a and b) describing the stability of the vortex tubes, analogous to Rayleigh-Bénard convection, that can be expected to play a major role in the flow. This is the model that one should simulate and analyze to get a better picture of the flow in the jet engine. However, we are not done if we also want to investigate how the conventional Moore-Greitzer equations fit into the new model and this is the topic for the next three sections.

10   The mean flow and the deviation

In this section, we are going to split the u_z equation into the mean flow and the deviation in order to compare with the Moore-Greitzer equation.

Consider the first two equations in (9.18). We integrate both of these equations with respect to the z variable imagining the compressor to be equivalent to an actuator disk. This was suggested by Moore and Greitzer, see [30]. Since we want to compare with the original Moore-Greitzer equation, we implement this idea by integration in z. The result is:

$$
\begin{cases}
\dfrac{\partial \overline{u_z^0}}{\partial \tau_s} = -(\nabla \hat{u}_z^0 \cdot \overline{\chi^z \otimes \chi^z} \cdot \nabla \hat{u}_z^0)|_{z_0}^{z_1} - \dfrac{(\hat{u}_z^0)^2}{2}|_{z_0}^{z_1} - \hat{p}_1|_{z_0}^{z_1} \\[3mm]
\dfrac{\partial \overline{a}}{\partial \tau_s} = -\overline{\hat{u}_z^0 \hat{a}}|_{z_0}^{z_1} - \left(\overline{\chi^z a \cdot \nabla \overline{u_z^0}} \right)|_{z_0}^{z_1} \\[3mm]
\dfrac{\partial \overline{b}}{\partial \tau_s} = -\overline{\hat{u}_z^0 \hat{b}}|_{z_0}^{z_1} - \left(\overline{\chi^z a \cdot \nabla \overline{u_z^0}} \right)|_{z_0}^{z_1},
\end{cases}
\tag{10.1}
$$

where z_0 marks the entrance and z_1 the exit of the compressor scaled by $\frac{L}{R}$.

We have redefined the meaning of the overlines to simplify notation. It is now redefined to be the mean over z, ζ, κ, α, τ_f and t wheras hat indicates the old overline that was the mean over ζ, κ, α, τ_f and t only. Moreover z has been rescaled by $\frac{L}{R}$.

Note that $\overline{\frac{\partial u_z^2}{\partial z}}$ and $\overline{\frac{\partial p_1}{\partial z}}$ are the same as the difference of the average of u_z^2 and p_1 respectively over local variables, fast and normal times evaluated at the two ends of the compressor. If we switch to the old definition of the overline, i.e., only the average over local variables, fast and normal times, we could rewrite these terms as $\overline{u_z^2}(z_1) - \overline{u_z^2}(z_0)$ and $\overline{p_1}(z_1) - \overline{p_1}(z_0)$, where z_1 is the back end of the compressor and z_0 is the front end.

We next make a closure ansatz analogous to the one in Section 7. We express the

previous average of the velocity $\hat{u}_z^0$ and amplitudes as,

$$\begin{cases} \hat{u}_z^0 = \overline{u_z^0} + \xi^z\left(z\right) \cdot \nabla \overline{u_z^0} \\[2mm] \hat{a} = \overline{a} + \xi^a\left(z\right) \cdot \nabla \overline{a} \\[2mm] \hat{b} = \overline{b} + \xi^b\left(z\right) \cdot \nabla \overline{b}. \end{cases} \tag{10.2}$$

A substitution of the expressions (10.2) into the equations (10.1) gives the new equation

$$\frac{\partial \overline{u_z^0}}{\partial \tau_s} = -2\nabla \hat{u}_z^0 \cdot \overline{\chi^z \otimes \chi^z} \cdot \nabla \left(E \cdot \nabla \overline{u_z^0}\right) \quad -\nabla\left(E \cdot \nabla \overline{u_z^0}\right) \cdot \overline{\chi^z \otimes \chi^z} \cdot \nabla \left(D \cdot \nabla \overline{u_z^0}\right) \tag{10.3}$$

$$-\frac{(\hat{u}_z^0)^2}{2}\big|_{z_0}^{z_1} - \hat{p}_1\big|_{z_0}^{z_1}, \tag{10.4}$$

where $E = \xi^z(z_1) - \xi^z(z_0)$ and $D = \xi^z(z_1) + \xi^z(z_0)$ and ∇ denotes the two-dimensional (r and θ) gradient. The amplitude equations can similarly be found but they are probably not physically relevant for the actuator disk model. We are going to use the equation (10.3) to compare with the Moore-Greitzer equation but whereas the first term of the right is a viscous term, we have to discuss the role of the last three terms.
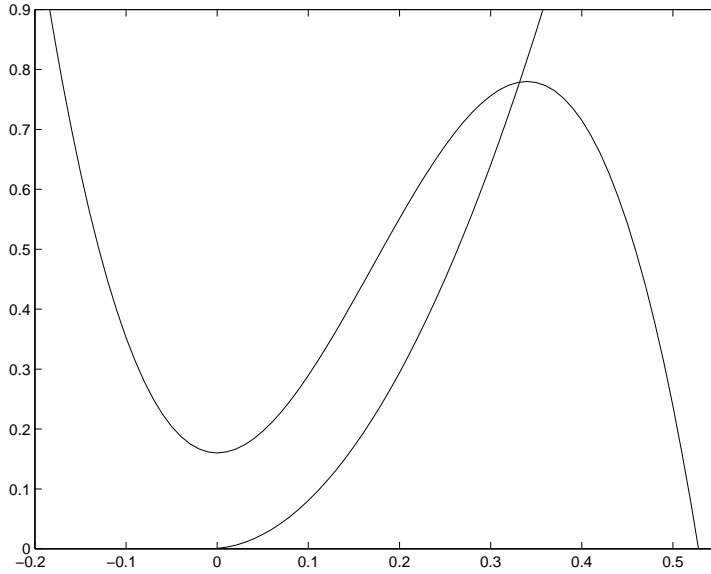

Figure 4: The Pressure Characteristic and the Throttle Curve (passing through the origin), the vertical axis is the pressure rise Ψ, and the horizontal axis is the mean flow Φ.

Let Ψ be the pressure rise from the plenum to the throttle, which is independent of θ (This will be discussed below). Then motivated by the equation (10.3) we can define the total pressure rise in the compressor as well as in the plenum.

Definition 10.1 *The pressure characteristic is defined to be*

$$\psi_c = \frac{R}{L}\left(\overline{p_1}(z_0) - \overline{p_1}(z_1)\right) + \frac{R}{2L}\left(u_z^2(z_1) - u_z^2(z_0)\right) - \nabla\left(E\cdot\nabla\overline{u}_z^0\right)\cdot\overline{\chi^z\otimes\chi^z}\cdot\nabla\left(D\cdot\nabla\overline{u}_z^0\right) + \Psi,$$

where the bar on $\overline{u}_z^0$ denotes the average over the local variables, fast time and z. Notice that we have reverted back to the unscaled z variable in the definition. The conventional model for the pressure characteristic is exhibited in Figure 4.

We now take the θ average and split the $\overline{u}_z^0$ equation into the mean flow Φ over θ and the deviation φ from the mean:

$$\frac{\partial\varphi}{\partial\tau_s} = -2(\overline{\chi^z\chi_r^z}\frac{\partial\Phi}{\partial r} + \overline{\chi^z\otimes\chi^z}\cdot\nabla\varphi)\cdot\nabla\left(E\cdot\nabla\varphi\right) + \frac{1}{l_c}\left(\psi_c - \frac{1}{2\pi}\int_0^{2\pi}\psi_c d\theta\right)$$

$$\frac{\partial\Phi}{\partial\tau_s} = -2((\overline{\chi_r^z})^2\frac{\partial\Phi}{\partial r} + \overline{\chi^z\chi_r^z}\cdot\nabla\varphi)\frac{1}{r}\frac{\partial}{\partial r}\left(rE_r\frac{\partial\Phi}{\partial r}\right) + \frac{1}{l_c}\left(\frac{1}{2\pi}\int_0^{2\pi}\psi_c d\theta - \Psi\right) \qquad (10.5)$$

The two equations (10.5) give the equations for the deviation from the mean flow and mean flow respectively. Then we need just one more equation for the pressure rise Ψ to be able to compare with the viscous Moore-Greitzer system (1.1).

11   The equation for the pressure rise

In this section, we are going to discuss the equation for the pressure rise in the Moore-Greitzer equation.

The conservation of mass in the plenum gives the dynamic equation, see Moore and Greitzer [30], for the pressure rise from the plenum to the throttle:

$$\frac{\partial\Psi^\varepsilon}{\partial t} = \frac{1}{4l_c(B^\epsilon)^2}[\Phi^\varepsilon - \gamma F_T^{-1}(\Psi^\varepsilon)] \qquad (11.1)$$

where $l_c = \frac{L}{R}$, $B^\epsilon = \frac{U}{2a_s}\sqrt{\frac{V_p}{A_c^\epsilon L}}$, V_p is the volume of the plenum, $A_c^\epsilon = \epsilon 2\pi R$ is the cross-sectional area of the compressor, γ is the throttle parameter, $F_T^{-1}(\Psi^\epsilon) = sgn(\Psi^\epsilon)\sqrt{|\Psi^\epsilon|}$ and Ψ^ε is the pressure rise from the plenum to the throttle.

The mean flow Φ^ε in the compressor is proportional to the rate of mass coming into the plenum from the outlet duct. The throttle flow $\gamma F_T^{-1}(\Psi^\varepsilon)$ (where F_T is the parabolic throttle characteristic) is proportional to the rate of mass going out of the plenum through the throttle. The difference of these two rates will result in a change of density in the plenum. On the other hand, the isentropic relation between density and pressure provides that the rate of density change in the plenum is proportional to the rate of change of pressure rise in the plenum. The gas in the plenum acts as a dynamics spring and must therefore be taken to be compressible in distinction to the air in the compressor. For more details on how the above equation is derived, see [30].

We now make the following asymptotic expansion for the pressure rise:

$$\Psi^\varepsilon(r,\theta,t) = \sum_{i=1}^{\infty} \epsilon^i \Psi_i\left(r,\theta,\sqrt{\varepsilon}t, t, \frac{t}{\sqrt{\varepsilon}}\right). \tag{11.2}$$

Note that the expansion starts at $i = 1$ since the 0th order pressure is the ambient pressure which does not change from the inlet duct to the throttle and thus the 0th order pressure rise is zero. Applying the chain rule $\frac{\partial}{\partial t} = \sqrt{\varepsilon}\frac{\partial}{\partial \tau_s} + \frac{\partial}{\partial t} + \frac{1}{\sqrt{\epsilon}}\frac{\partial}{\partial \tau_f}$ and gathering terms of the same order gives for

$\varepsilon^{1/2}$:

$$\frac{\partial \Psi_1}{\partial \tau_f} = 0, \tag{11.3}$$

ε^1:

$$\frac{\partial \Psi_1}{\partial t} = 0, \tag{11.4}$$

$\varepsilon^{3/2}$:

$$\frac{\partial \Psi_1}{\partial \tau_s} + \frac{\partial \Psi_2}{\partial \tau_f} = \frac{1}{4l_c B^2}(\Phi_0 - \gamma\, sgn(\Psi_1)\sqrt{|\Psi_1|}), \tag{11.5}$$

where $B = \sqrt{\epsilon}B^\epsilon = \frac{U}{2a_s}\sqrt{\frac{V_p}{\pi R^2 L}}$. Averaging over the fast time gives

$$\frac{\partial \Psi}{\partial \tau_s} = \frac{1}{4l_c B^2}(\Phi - \gamma\, sgn(\Psi)\sqrt{|\Psi|}) \tag{11.6}$$

where Φ is the averaged Φ_0 and $\Psi = \Psi_1$, since (11.3) and (11.4) imply that the pressure rise is constant with respect to the fast and normal time.

In the paper [5] it was proven that the solutions of the ODEs for Φ and Ψ are bounded. This permits us to apply the formal stochastic homogenization to Ψ^ϵ along with its application to the air velocity u^ϵ.

12 The modified Moore-Greitzer equation

Combining the equations in the previous two sections, we have the following system:

$$\begin{cases} \dfrac{\partial \varphi}{\partial \tau_s} = -2(\overline{\chi^z\chi_r^z}\dfrac{\partial \Phi}{\partial r} + \overline{\chi^z\otimes\chi^z}\cdot\nabla\varphi)\cdot\nabla(E\cdot\nabla\varphi) + \dfrac{1}{l_c}\left(\psi_c - \dfrac{1}{2\pi}\int_0^{2\pi}\psi_c d\theta\right) \\[3mm] \dfrac{\partial \Phi}{\partial \tau_s} = -2((\overline{\chi_r^z})^2\dfrac{\partial \Phi}{\partial r} + \overline{\chi^z\chi_r^z}\cdot\nabla\varphi)\dfrac{1}{r}\dfrac{\partial}{\partial r}\left(rE_r\dfrac{\partial \Phi}{\partial r}\right) + \dfrac{1}{l_c}\left(\dfrac{1}{2\pi}\int_0^{2\pi}\psi_c d\theta - \Psi\right) \\[3mm] \qquad\qquad \dfrac{\partial \Psi}{\partial \tau_s} = \dfrac{1}{4l_c B^2}(\Phi - \gamma\, sgn(\Psi)\sqrt{|\Psi|}) \end{cases} \tag{12.1}$$

27

where the coefficients of the eddy viscosity matrix are listed in Appendix B. This is the modified Moore-Greitzer we derived from the Navier-Stokes equations using stochastic homogenization. Compared with the original Moore-Greitzer equation, the difference is as follows:

First, the form of the eddy viscosity term is generalized. We showed that it is not just the second derivative with respect to θ as in the original Moore-Greitzer equation, it does have radial derivatives as well, only when there is negligible flow in the r direction in the compressor will the simple eddy viscosity term in the Moore-Greitzer equation be a good model.

Secondly, the forcing term ψ_c is given explicitly in Definition 10.1, while the original assumption was to model it using a cubic polynomial of the velocity in z direction. p_1 could be found by solving the Poisson equation for the pressure as explained in Section 7, $u_z^2(z_1) = g_{out}^0$ and $u_z^2(z_0) = g_{in}^0$ are given by the boundary conditions in the outlet and inlet ducts.

Recall that if we used the frame rotating with the speed of the rotors instead of half the speed of the rotors, we will have a first θ-derivative term in the deviation equation. If we transfer from our frame moving with half the speed of the rotors, to the inertial frame of reference, where $\frac{\partial \varphi}{\partial \tau} = \frac{\partial \varphi}{\partial \tau_s} + \frac{1}{2}\frac{\partial \varphi}{\partial \theta}$, then the (slightly) improved Moore-Greitzer system becomes:

The Modified Viscous Moore-Greitzer Equation

$$
\begin{cases}
\dfrac{\partial \varphi}{\partial \tau_s} = -2(\overline{\chi^z \chi_r^z}\dfrac{\partial \Phi}{\partial r} + \overline{\chi^z \otimes \chi^z} \cdot \nabla\varphi) \cdot \nabla(E \cdot \nabla\varphi) - \dfrac{1}{2}\dfrac{\partial \varphi}{\partial \theta} + \dfrac{1}{l_c}\left(\psi_c - \dfrac{1}{2\pi}\int_0^{2\pi}\psi_c d\theta\right) \\[4mm]
\dfrac{\partial \Phi}{\partial \tau_s} = -2((\overline{\chi_r^z})^2\dfrac{\partial \Phi}{\partial r} + \overline{\chi^z \chi_r^z} \cdot \nabla\varphi)\dfrac{1}{r}\dfrac{\partial}{\partial r}\left(rE_r\dfrac{\partial \Phi}{\partial r}\right) + \dfrac{1}{l_c}\left(\dfrac{1}{2\pi}\int_0^{2\pi}\psi_c d\theta - \Psi\right) \\[4mm]
\dfrac{\partial \Psi}{\partial \tau_s} = \dfrac{1}{4l_c B^2}(\Phi - \gamma\, sgn(\Psi)\sqrt{|\Psi|})
\end{cases}
$$

$$(12.2)$$

Finally, we prove the second part of our main result:

Theorem 12.1 *The mean flow Φ plus the deviation φ, in the solution to the modified viscous Moore-Greitzer equation (12.2), is the z and normal-time t average of the formal homogenized* [2] *limit*

$$\int_{z_0}^{z_1} \hat{u}_z^0 dz = \Phi + \varphi,$$

of (the z component of) the solution $\epsilon^{-1/2} \cdot u^\epsilon$, to the Navier-Stokes equation (2.1), as $\epsilon \to 0$.

---

[2]averaged over the fast time and spatially local variables

Proof: We obtain from Theorem 9.1 that formally $\epsilon^{-1/2} \cdot u^\epsilon \to \overline{u}^0$, where u^0 solves the global homogenized Navier-Stokes equation (9.18). It follows that $\overline{u}_z^0$ is the stochastically homogenized formal limit of $\epsilon^{-1/2} \cdot u_z^\epsilon$. After we have integrated with respect to z from z_0 to z_1, and averaged over the normal time as in Equation (9.18), where hat now denotes the average over normal time, we obtain

$$\hat{u}_z^0 = \frac{1}{2\pi} \int_0^{2\pi} \overline{u}_z^0 dt.$$

Then we split $\int_{z_0}^{z_1} \overline{u}_z^0 dz = \Phi + \varphi$ as in Section 10, see Equation (10.5) and add Equation (11.6) from Section 11 to get the modified viscous Moore-Greitzer equation (12.2). **QED**

Corollary 12.1 *If the radial components of the eddy viscosity are small, then the original viscous Moore-Greitzer equation (1.1) is an excellent approximation to the modified viscous Moore-Greitzer equation (12.2).*

Proof: Assume that the r derivatives of φ and Φ are small. Then neglecting those terms in Equation (12.2) we get

$$
\begin{cases}
\dfrac{\partial \varphi}{\partial \tau_s} = -\dfrac{2\overline{\chi_\theta^z \chi_r^z}}{r^3} \dfrac{\partial \varphi}{\partial \theta} \dfrac{\partial}{\partial \theta} \left(E_\theta \dfrac{\partial \varphi}{\partial \theta} \right) - \dfrac{1}{2} \dfrac{\partial \varphi}{\partial \theta} + \dfrac{1}{l_c} \left(\psi_c - \hat{\psi}_c \right) \\[4mm]
\dfrac{\partial \Phi}{\partial \tau_s} = \dfrac{1}{l_c} (\hat{\psi}_c - \Psi) \\[4mm]
\dfrac{\partial \Psi}{\partial \tau_s} = \dfrac{1}{4 l_c B^2} (\Phi - \gamma \, sgn(\Psi) \sqrt{|\Psi|}),
\end{cases}
\tag{12.3}
$$

This is the viscous Moore-Greitzer equation with the viscosity coefficient,

$$-\frac{2\overline{\chi_\theta^z \chi_r^z}}{r^3} E_\theta > 0.$$

Recall that here $\overline{\chi_\theta^z \chi_r^z} E_\theta$ are averaged over the small spatial scales, fast and normal time, so the product is a constant. Thus if the r derivatives of φ and Φ are small we recover the viscous Moore-Greitzer equation (1.1) with the viscous term

$$-\frac{2\overline{\chi_\theta^z \chi_r^z}}{r^3} \frac{\partial \varphi}{\partial \theta} \frac{\partial}{\partial \theta} \left(E_\theta \frac{\partial \varphi}{\partial \theta} \right)$$

as suggested in [1] and [26]. **QED**

Remark 12.1 The explicit form of the pressure characteristic in Definition 10.1 shows that it is probably not enough to model the pressure characteristic as a function of $\overline{u}_z^0$ only. Even if the first two terms can be modeled in this way the third term is a function of the gradient $\nabla \overline{u}_z^0$.

29

13   Coupling to a Combustion Model

In this section we discuss how the above results and in particular the improved model (9.18) can be coupled to a detailed combustion model for the combuster and afterburner in a jet engine.

In flows with density changes as occur in combustion one introduces a density-weighted average $\overline{u}$, called the Favre average, thus splitting the fluid velocity into the average and the deviation

$$u(x, t) = \overline{u}(x, t) + \hat{u}(x, t).$$

The averaged continuity and momentum equations become

The Favre averaged continuity equation

$$\frac{\partial \overline{\rho}}{\partial t} + \bigtriangledown \cdot (\overline{\rho u}) = 0, \tag{13.4}$$

and

The Favre averaged momentum equation

$$\frac{\partial (\overline{\rho u})}{\partial t} + \bigtriangledown \cdot (\overline{\rho u} \otimes \overline{u}) - \bigtriangledown \cdot \overline{\tau} + \bigtriangledown \cdot (\overline{\rho} \hat{u} \otimes \hat{u}) = -\bigtriangledown \overline{p} + \overline{\rho} g, \tag{13.5}$$

where the term $(\overline{\rho} \hat{u} \otimes \hat{u})$ is called the Reynolds stress tensor. These equations are used to derive equations for the Favre averaged turbulent kinetic energy k, and the Favre averaged turbulent dissipation ϵ. The resulting equations depend on the model of the Reynolds stress tensor and are referred to as k-ϵ models, see [32]. In addition, one needs an equation for the Favre averaged mixture fraction

The mixture fraction equation

$$\overline{\rho}\frac{\partial z}{\partial t} + \overline{\rho u} \cdot \bigtriangledown z = \bigtriangledown \cdot (\overline{\rho} D \bigtriangledown z), \tag{13.6}$$

where D is the diffusion coefficient and

$$z = \frac{\eta Y_F - Y_{O_2} + Y_{O_{2A}}}{\eta Y_{F_1} - Y_{O_{2,A}}}$$

is the mixture fraction of fuel and oxygen O_2, Y_F being the mass of the fuel and Y_{O_2} that of the oxygen, at any give time, and Y_{F_1} being the mass of the fuel and $Y_{O_{2,A}}$ the mass of the oxygen, in the fuel and oxidizer stream respectively and η is the stoichiometric oxygen-to-fuel mass ratio. One also needs equations for the mass fractions Y_i of all the chemical species involved in the reaction. There remains one equation the *enthalpy equation*, but with some simplifying assumptions, [32], it becomes the same as the mixture fraction equation (13.6).

One can use the same approach as we used to get the effective equations for the compressor, in this paper, to get the effective equations for the combustion in the plenum

and the afterburners. The full system of equations is too complicated to be analyzed by current technology but there is a well developed theory of one-dimensional thermal shocks propagating trough a fuel mixture. One can now hope to make the connection between the effective equations and this theory and perhaps bring the latter to bear on the observed longitudinal and azimuthal thermoacoustic instabilities in the combustor and afterburners. If these phenomena cannot be reduced to one-dimensional shock waves the resulting equations may still have to be solved numerically. Finally, the flow determined by (9.18) can be fed into these equations and the effective combustion studied. One does not expect the spatial structure of the disturbances, surge and stall, to be important. These details will be washed out in the overwhelming mass of the plenum. However, the flow disturbances will show up in fluctuation in the mean flow and swirl and these will affect the combustion and possibly the shock formation.

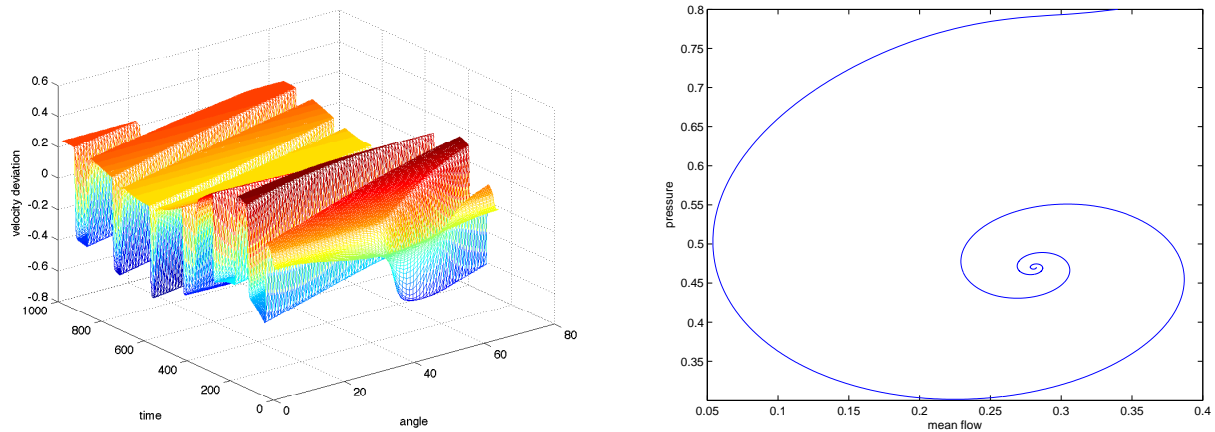# 14 A Numerical Comparison of the Viscous Moore-Greitzer Equation and the New Model

Figure 5: The deviation from the mean flow and the pressure as a function of mean flow during the initiation and propogation of a stall cell

We can now simulate the new equations and compare the results with the solutions of the viscous Moore-Greitzer equations (1.1). First we will simulate the equations (12.3), in the following form that we will call the New Model 1:

New Model 1

$$
\begin{cases}
\dfrac{\partial \varphi}{\partial \tau_s} = \nu \left| \dfrac{\partial \varphi}{\partial \theta} \right| \left(\dfrac{\partial^2 \varphi}{\partial \theta^2} \right) - \dfrac{1}{2} \dfrac{\partial \varphi}{\partial \theta} + \dfrac{1}{l_c} \left(\psi_c - \hat{\psi}_c \right) \\[3mm]
\qquad\qquad \dfrac{\partial \Phi}{\partial \tau_s} = \dfrac{1}{l_c} (\hat{\psi}_c - \Psi) \\[3mm]
\quad \dfrac{\partial \Psi}{\partial \tau_s} = \dfrac{1}{4 l_c B^2} (\Phi - \gamma \, sgn(\Psi) \sqrt{| \Psi |}),
\end{cases}
\tag{14.7}
$$

These equations are the same as the viscous Moore-Greitzer equations (1.1) except for the derivative $\frac{\partial \varphi}{\partial \theta}$ multiplying the viscous term $\frac{\partial^2 \varphi}{\partial \theta^2}$. In Figures 5 to 7, we simulate the initiation and propagation of stall, first without and then with control, and then a surge cycle, without and with control (in Figure 7). The parameter values are the same as in [6]. A comparison between these simulations and those in [7] and [6] show that there is now difference between the solutions of the New Model 1 and the viscous Moore-Greitzer equations with or without basic control, see [6] and [8]. In these figures the stall cell is seen in the plot of the deviation from the mean flow plotted as a function of angle and time, and the pressure is plotted against the mean flow on a separate plot. The conclusion of this simulation is that the term $\frac{\partial \varphi}{\partial \theta}$ makes only a slight quantitative and no qualitative difference.
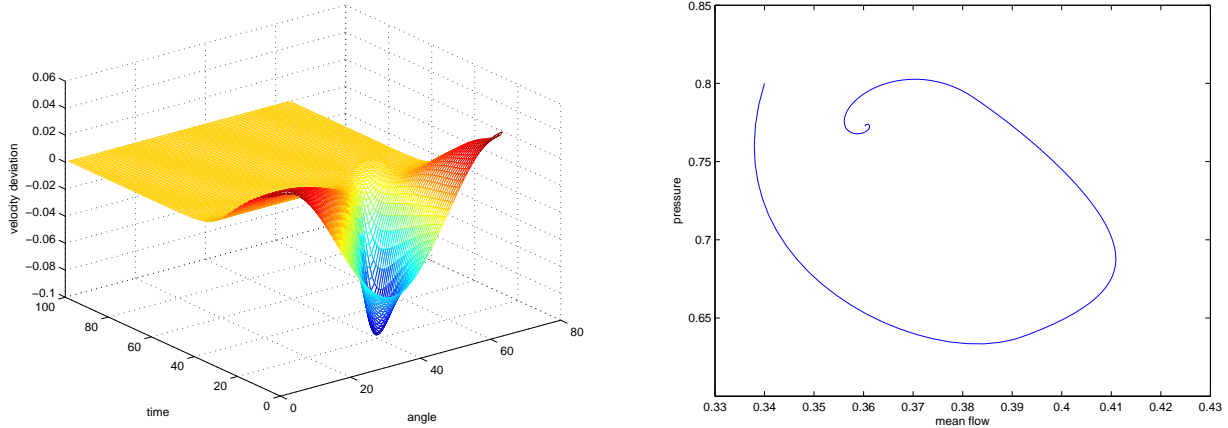

Figure 6: The deviation from the mean flow and the pressure as a function of mean flow when the initiation of a stall cell is quenched by control.

Next we will simulate a more general form of the new model (9.18), in a modified form of the equations (12.2) that we will call the New Model 2:
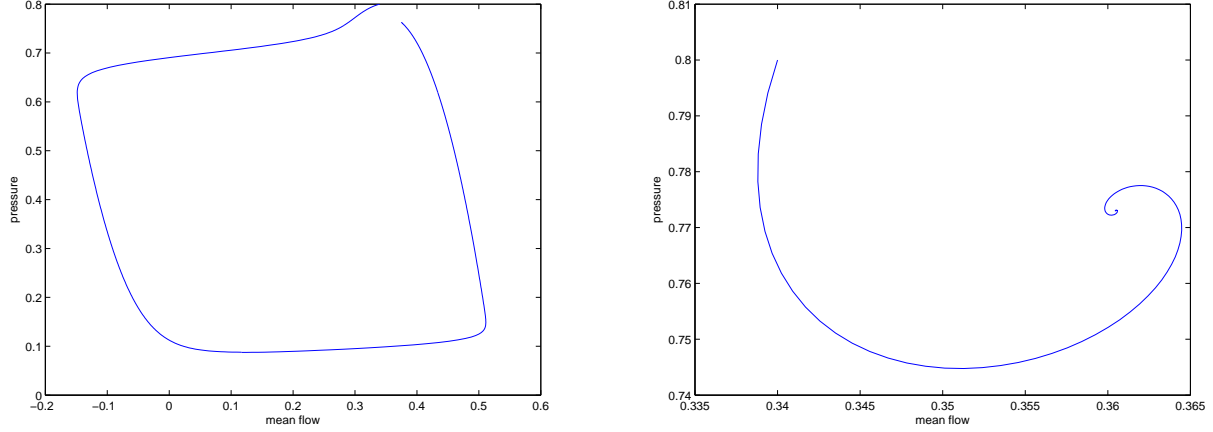
Figure 7: The pressure as a function of mean flow during a surge cycle and (on right) the control of the surge.

New Model 2

$$
\begin{cases}
\dfrac{\partial \varphi}{\partial \tau_s} = \nu(|\dfrac{\partial \varphi}{\partial \theta}| + b|\dfrac{\partial \Phi}{\partial r}|)\left(\dfrac{\partial^2 \varphi}{\partial \theta^2}\right) - \dfrac{1}{2}\dfrac{\partial \varphi}{\partial \theta} + \dfrac{1}{l_c}\left(\psi_c - \dfrac{1}{2\pi}\int_0^{2\pi}\psi_c d\theta\right) \\[4mm]
\dfrac{\partial \Phi}{\partial \tau_s} = a|\dfrac{\partial \Phi}{\partial r}|\dfrac{1}{r}\dfrac{\partial}{\partial r}\left(r\dfrac{\partial \Phi}{\partial r}\right) + \dfrac{1}{l_c}\left(\dfrac{1}{2\pi}\int_0^{2\pi}\psi_c d\theta - \Psi\right) \\[4mm]
\dfrac{\partial \Psi}{\partial \tau_s} = \dfrac{1}{4l_c B^2}(\Phi - \gamma\, sgn(\Psi)\sqrt{|\Psi|})
\end{cases}
\tag{14.8}
$$

In this model we have ignored the radial derivative of the deviation φ assuming that it is small compared to the radial derivative of the mean flow Φ. The parameter values are the same as in [6], except for the new parameters $a = 0.001$, $b = 0.5$. The solutions of these equations are more complicated that the solutions of the viscous Moore-Greitzer equations (1.1). Firstly, they depend on the radial direction in the compressor as shown in Figure 8. This figure shows the mean flow as a function of radius and time (left) and then a stall cell as a function of angle and radius for a fixed time (right). We see that the mean flow has radial dependance increasing at the outer boundary and the stall cell, while being reasonably uniform in the radial directions develops spatial oscillations in its angular wings. In comparison the wings of the Moore-Greitzer stall cell are uniform. The viscous Moore-Greitzer stall cell (left) is compared with a cut of the stall cell of New Model 2 (right) at $r = 1$ in Figure 9. Secondly, it is clear from Figure 9 that the stall cell of the New Model 2 is a much more complicated and higher dimensional phenomenon than the stall cell of the viscous Moore-Greitzer equations (or New Model 1). Not surprisingly it is also much harder to control.
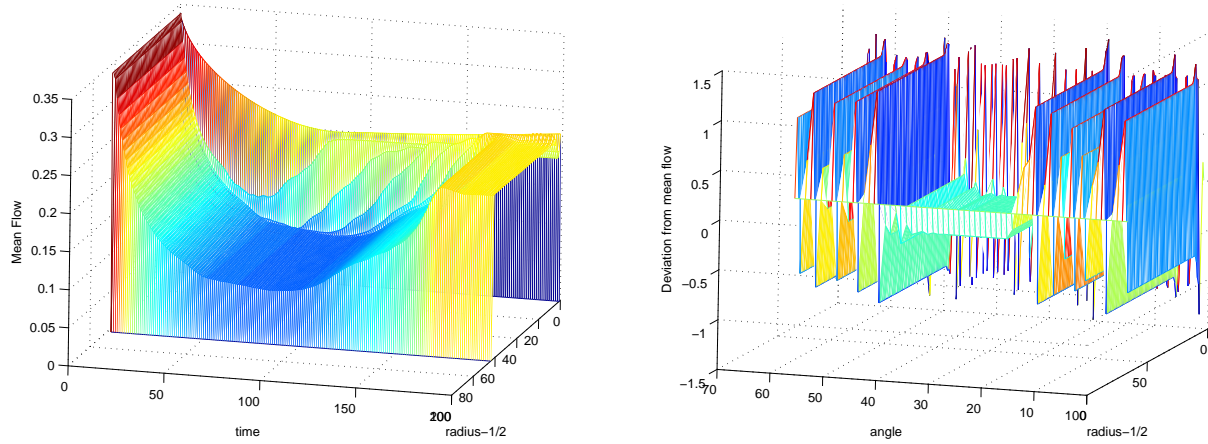
33

Figure 8: The mean flow as a function of time and radius and the deviation from the mean flow, at a fixed time during the stall cycle, for the New Model 2.
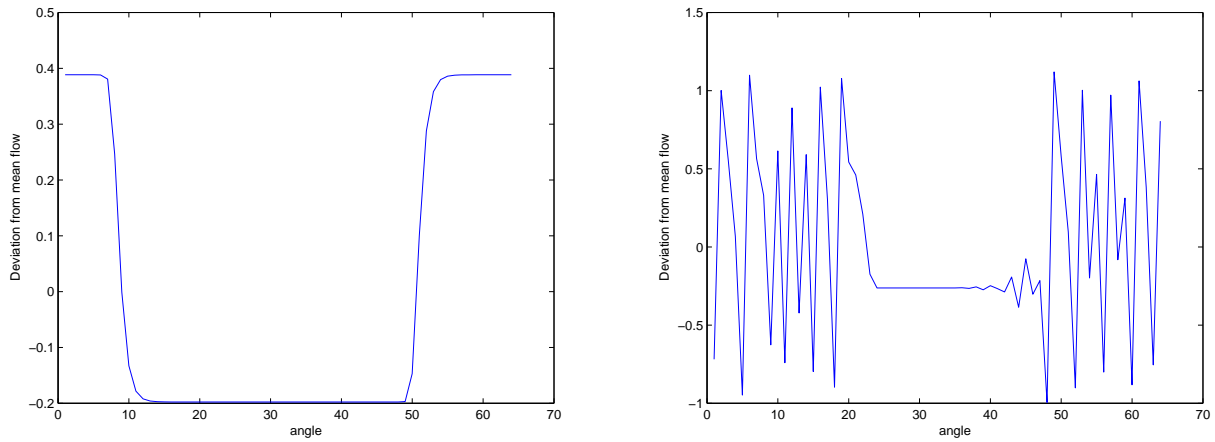

Figure 9: The viscous Moore-Greitzer stall cell (left) compared with a section of the stall cell of the New Model 2 (right).

34

A complete numerical analysis of the new model (9.18) is more complicated and will be done in another publication. In particular one has to include the equations determining the fluctuations in the swirl and its instabilities.

15   Conclusion

A homogenization of the incompressible Navier-Stokes equations assuming a stochastic homogenization theorem gives a derivation of the viscous Moore-Greitzer equations. A more general system of equations was obtained containing the viscous Moore-Greitzer equations as a special case. This more general system of the equations called the New Model (9.18) give a much better description of the flow through the compressor and the instabilities surge and stall in that flow. In addition equations are obtained describing the swirl of the flow that is the only spatial structure of the flow that persists in the plenum.

A full numerical analysis of the New Model (9.18) remains to be done but special cases that arise when the swirl is ignored and certain approximations implemented give respectively agreement with the viscous Moore-Greitzer model (New Model 1 (14.7)) and a generalization of it (New Model 2 (14.8)), revealing more complicated structure of stall and implying that stall is harder to control than previously known. The New Model (9.18) opens the prospect of a complete controllability of instabilities in the compressor and the extension of active control of flow and combustion in whole jet engine, including control of thermoacoustic instabilities in the plenum and afterburners.

The New Model 2 (14.8) seems to be a better description of what actually goes on in the compressor than the viscous Moore-Greitzer equations (1.1) and more useful in designing controls that can be implemented in real time. It is likely that the full New Model (9.18) will give even more information and more effective control methods.

A   The Global Equations

The ϵ^1 terms in the asymptotic expansion (4.1) give us the global slow time Navier-Stokes equation:

$$
\begin{cases}
\dfrac{\partial u_z^0}{\partial \tau_s} + \dfrac{\partial u_z^1}{\partial \tau_f} + u_r^0\dfrac{\partial u_z^0}{\partial r} + u_r^0\dfrac{\partial u_z^1}{\partial \alpha} + u_r^1\dfrac{\partial u_z^0}{\partial \alpha} + \dfrac{1}{r}\left(u_\theta^0\dfrac{\partial u_z^0}{\partial \theta} + u_\theta^0\dfrac{\partial u_z^1}{\partial \kappa} + u_\theta^1\dfrac{\partial u_z^0}{\partial \kappa}\right) \\[2mm]
\qquad\qquad + \dfrac{R}{L}\left(u_z^0\dfrac{\partial u_z^0}{\partial z} + u_z^0\dfrac{\partial u_z^1}{\partial \zeta} + u_z^1\dfrac{\partial u_z^0}{\partial \zeta}\right) \\[2mm]
-\dfrac{\nu}{\beta R^2}\left(\dfrac{1}{r}\dfrac{\partial u_z^0}{\partial \alpha} + \dfrac{\partial^2 u_z^0}{\partial r\partial \alpha} + \dfrac{\partial^2 u_z^0}{\partial \alpha\partial r} + \dfrac{\partial^2 u_z^1}{\partial \alpha^2} + \dfrac{1}{r^2}\left(\dfrac{\partial^2 u_z^0}{\partial \theta\partial \kappa} + \dfrac{\partial^2 u_z^0}{\partial \kappa\partial \theta} + \dfrac{\partial^2 u_z^1}{\partial \kappa^2}\right)\right) \\[2mm]
\qquad\qquad -\dfrac{\nu}{\beta L^2}\left(\dfrac{\partial^2 u_z^0}{\partial z\partial \zeta} + \dfrac{\partial^2 u_z^0}{\partial \zeta\partial z} + \dfrac{\partial^2 u_z^1}{\partial \zeta^2}\right) = -\dfrac{R}{L}\left(\dfrac{\partial p_1}{\partial z} + \dfrac{\partial p_2}{\partial \zeta}\right), \\[4mm]
\dfrac{\partial u_r^0}{\partial \tau_s} + \dfrac{\partial u_r^1}{\partial \tau_f} + u_r^0\dfrac{\partial u_r^0}{\partial r} + u_r^0\dfrac{\partial u_r^1}{\partial \alpha} + u_r^1\dfrac{\partial u_r^0}{\partial \alpha} + \dfrac{1}{r}\left(u_\theta^0\dfrac{\partial u_r^0}{\partial \theta} + u_\theta^0\dfrac{\partial u_r^1}{\partial \kappa} + u_\theta^1\dfrac{\partial u_r^0}{\partial \kappa}\right) \\[2mm]
\qquad\qquad -\dfrac{1}{r}\left(u_\theta^0\right)^2 + \dfrac{R}{L}\left(u_z^0\,\dfrac{\partial u_r^0}{\partial z} + u_z^0\dfrac{\partial u_r^1}{\partial \zeta} + u_z^1\dfrac{\partial u_r^0}{\partial \zeta}\right) \\[2mm]
-\dfrac{\nu}{\beta R^2}\left(\dfrac{1}{r}\dfrac{\partial u_r^0}{\partial \alpha} + \dfrac{\partial^2 u_r^0}{\partial r\partial \alpha} + \dfrac{\partial^2 u_r^0}{\partial \alpha\partial r} + \dfrac{\partial^2 u_r^1}{\partial \alpha^2} + \dfrac{1}{r^2}\left(\dfrac{\partial^2 u_r^0}{\partial \theta\partial \kappa} + \dfrac{\partial^2 u_r^0}{\partial \kappa\partial \theta} + \dfrac{\partial^2 u_r^1}{\partial \kappa^2}\right)\right) \\[2mm]
\qquad\qquad -\dfrac{\nu}{\beta L^2}\left(\dfrac{\partial^2 u_r^0}{\partial z\partial \zeta} + \dfrac{\partial^2 u_r^0}{\partial \zeta\partial z} + \dfrac{\partial^2 u_r^1}{\partial \zeta^2}\right) = -\left(\dfrac{\partial p_1}{\partial r} + \dfrac{\partial p_2}{\partial \alpha}\right), \\[4mm]
\dfrac{\partial u_\theta^0}{\partial \tau_s} + \dfrac{\partial u_\theta^1}{\partial \tau_f} + u_r^0\dfrac{\partial u_\theta^0}{\partial r} + u_r^0\dfrac{\partial u_\theta^1}{\partial \alpha} + u_r^1\dfrac{\partial u_\theta^0}{\partial \alpha} + \dfrac{1}{r}\left(u_\theta^0\,\dfrac{\partial u_\theta^0}{\partial \theta} + u_\theta^0\dfrac{\partial u_\theta^1}{\partial \kappa} + u_\theta^1\dfrac{\partial u_\theta^0}{\partial \kappa}\right) \\[2mm]
\qquad\qquad + \dfrac{1}{r}u_r^0 u_\theta^0 + \dfrac{R}{L}\left(u_z^0\dfrac{\partial u_\theta^0}{\partial z} + u_z^0\dfrac{\partial u_\theta^1}{\partial \zeta} + u_z^1\dfrac{\partial u_\theta^0}{\partial \zeta}\right) \\[2mm]
-\dfrac{\nu}{\beta R^2}\left(\dfrac{1}{r}\dfrac{\partial u_\theta^0}{\partial \alpha} + \dfrac{\partial^2 u_\theta^0}{\partial r\partial \alpha} + \dfrac{\partial^2 u_\theta^0}{\partial \alpha\partial r} + \dfrac{\partial^2 u_\theta^1}{\partial \alpha^2} + \dfrac{1}{r^2}\left(\dfrac{\partial^2 u_\theta^0}{\partial \theta\partial \kappa} + \dfrac{\partial^2 u_\theta^0}{\partial \kappa\partial \theta} + \dfrac{\partial^2 u_\theta^1}{\partial \kappa^2}\right)\right) \\[2mm]
\qquad\qquad -\dfrac{\nu}{\beta L^2}\left(\dfrac{\partial^2 u_\theta^0}{\partial z\partial \zeta} + \dfrac{\partial^2 u_\theta^0}{\partial \zeta\partial z} + \dfrac{\partial^2 u_\theta^1}{\partial \zeta^2}\right) = -\dfrac{1}{r}\left(\dfrac{\partial p_1}{\partial \theta} + \dfrac{\partial p_2}{\partial \kappa}\right).
\end{cases}
\tag{A.9}
$$

This system describes the velocity field in both the large and the small scales.

B   The Eddy Viscosity Tensor

The eddy viscosity coefficients for the equations (7.6),(7.8) and (7.10) in Section 7 are:

$$
\begin{cases}
a_{11} = -\dfrac{R}{L}\overline{\chi_z^z \chi^z} \cdot \bigtriangledown \overline{u_z^0}, & a_{12} = -\dfrac{R}{L}\overline{\chi_\theta^z \chi^z} \cdot \bigtriangledown \overline{u_z^0}, & a_{13} = -\dfrac{R}{L}\overline{\chi_r^z \chi^z} \cdot \bigtriangledown \overline{u_z^0} \\[2mm]
a_{21} = -\overline{\chi_z^z \chi^r} \cdot \bigtriangledown \overline{u_r^0}, & a_{22} = -\overline{\chi_\theta^z \chi^r} \cdot \bigtriangledown \overline{u_r^0}, & a_{23} = -\overline{\chi_r^z \chi^r} \cdot \bigtriangledown \overline{u_r^0} \\[2mm]
a_{31} = -\overline{\chi_z^z \chi^\theta} \cdot \bigtriangledown \overline{u_\theta^0}, & a_{32} = -\overline{\chi_\theta^z \chi^\theta} \cdot \bigtriangledown \overline{u_\theta^0}, & a_{33} = -\overline{\chi_r^z \chi^\theta} \cdot \bigtriangledown \overline{u_\theta^0},
\end{cases}
\tag{B.10}
$$

$$
\begin{cases}
b_{11} = -\dfrac{R}{L}\overline{\chi_z^r \chi^z} \cdot \bigtriangledown \overline{u_z^0}, & b_{12} = -\dfrac{R}{L}\overline{\chi_\theta^r \chi^z} \cdot \bigtriangledown \overline{u_z^0}, & b_{13} = -\dfrac{R}{L}\overline{\chi_r^r \chi^z} \cdot \bigtriangledown \overline{u_z^0} \\[2mm]
b_{21} = -\overline{\chi_z^r \chi^r} \cdot \bigtriangledown \overline{u_r^0}, & b_{22} = -\overline{\chi_\theta^r \chi^r} \cdot \bigtriangledown \overline{u_r^0}, & b_{23} = -\overline{\chi_r^r \chi^r} \cdot \bigtriangledown \overline{u_r^0} \\[2mm]
b_{31} = -\overline{\chi_z^r \chi^\theta} \cdot \bigtriangledown \overline{u_\theta^0}, & b_{32} = -\overline{\chi_\theta^r \chi^\theta} \cdot \bigtriangledown \overline{u_\theta^0}, & b_{33} = -\overline{\chi_r^r \chi^\theta} \cdot \bigtriangledown \overline{u_\theta^0},
\end{cases}
\tag{B.11}
$$

$$
\begin{cases}
c_{11} = -\dfrac{R}{L}\overline{\chi_z^\theta \chi^z} \cdot \bigtriangledown \overline{u_z^0}, & c_{12} = -\dfrac{R}{L}\overline{\chi_\theta^\theta \chi^z} \cdot \bigtriangledown \overline{u_z^0}, & c_{13} = -\dfrac{R}{L}\overline{\chi_r^\theta \chi^z} \cdot \bigtriangledown \overline{u_z^0} \\[2mm]
c_{21} = -\overline{\chi_z^\theta \chi^r} \cdot \bigtriangledown \overline{u_r^0}, & c_{22} = -\overline{\chi_\theta^\theta \chi^r} \cdot \bigtriangledown \overline{u_r^0}, & c_{23} = -\overline{\chi_r^\theta \chi^r} \cdot \bigtriangledown \overline{u_r^0} \\[2mm]
c_{31} = -\overline{\chi_z^\theta \chi^\theta} \cdot \bigtriangledown \overline{u_\theta^0}, & c_{32} = -\overline{\chi_\theta^\theta \chi^\theta} \cdot \bigtriangledown \overline{u_\theta^0}, & c_{33} = -\overline{\chi_r^\theta \chi^\theta} \cdot \bigtriangledown \overline{u_\theta^0}.
\end{cases}
\tag{B.12}
$$

References

[1] R.A. Adomaitis and E.H. Abed. Local nonlinear control of stall inception in axial flow compressors. *29th Joint Propulsion Conference and Exhibit*, 1993. AIAA Paper 93–2230.

[2] A. Banaszuk, H.A. Hauksson, and I. Mezić. A backstepping controller for a nonlinear partial differential equation model of compression system instabilities. *SIAM J. of Control and Optimization*, 37(5):1503–1537, 1999.

[3] B.Birnir and R.Grauer. The global attractor of the damped and driven sine-Gordon equation. *Comm. Math. Phys.*, 162:539–590, 1994.

[4] B. Birnir. *Basic Attractors and Basic Control of Nonlinear Partial Differential Equations*. ECMI Lecture Notes, Chalmers University of Technology and Göteborg University, 2001.

[5] B. Birnir and H.A. Hauksson. Finite dimensional attractor of the Moore-Greitzer PDE model. *SIAM J. of Applied Math.*, 59(2):636–650, 1998.

[6] B. Birnir and H.A. Hauksson. The basic control of the viscous Moore-Greitzer PDE model. *SIAM Journ. Control and Optimization*, 38(5):1554–1558, 2000.

[7] B. Birnir and H.A. Hauksson. The basic attractor of the viscous Moore-Greitzer PDE equation. *J. Nonlinear Sci.*, 11(2):169–192, 2001.

[8] B. Birnir and H.A. Hauksson. Basic dynamical systems control of aeroengine flow. In *Proceedings of the 39th IEEE CDC conference, Sidney Des. 2000*, New Jersey, 2001. IEEE.

[9] B. Birnir and N. Svanstedt. Existance and homogenization of the Rayleigh-Benard problem. *J. Nonl. Math. Phys.*, 7(2):136–169, 2000.

[10] Björn Birnir. Turbulent Rivers. *Submitted*, 2006. Available at: http:://www.math.ucsb.edu/~birnir/papers.

[11] Y. Chung and E. Titi. *Inertial Manifolds and Gevrey Regularity for the Moore-Greitzer Model of Turbo-Machine Engines.* To appear in J. Nonlin. Sci. 2002.

[12] D. Fontaine. Control of an axial flow compressor. Technical report, CCEC, UCSB, 2000.

[13] E.M. Greitzer. Surge and rotating stall in axial flow compressors: Part 2. *Trans. ASME Journal Engineering for Power*, Vol. 98:190–217, 1976.

[14] G. Hagen. *Large Scale Flow Fhenomena in Axial Compressors: Modeling, Analysis and Control with Air Injectors.* UCSB Ph.D. thesis, 2000.

[15] S. Hou. *Solutions of Multidimensional Hyperbolic Systems of Conservation Laws by Discontinuous Galerkin Methods and a Derivation of the Moore-Greitzer Equation using Homogenization.* UCSB Ph.D. thesis, 2003.

[16] J.S. Humbert and A.J. Krener. Analysis of higher order Moore-Greitzer compressor models. *IEEE Conference on Control Applications*, 1997.

[17] J.S. Humbert and A.J. Krener. Dynamics and control of entrained solutions in multi-mode Moore-Greitzer compressor models. *Int. J. Control*, 71(5):807–821, 1998.

[18] R.H. Kraichnan. Eddy viscosity in two and three dimensions. *J. Atmos. Sci.*, 33:1521–1536, 1976.

[19] H-O Kreiss and J. Lorenz. *Initial Value Problems and the Navier-Stokes Equations.* Academic Press, 1989.

[20] L.D. Landau and E.M. Lifshitz. *Fluid Mechanics*. Number 6 in Course in Theoretical Physics. Pergamon, New York, 1987.

[21] P. L. Lavrich. Time resolved measurements of rotation stall in axial flow compressors. MIT Department of Aeronautics and Astronautics, Ph.D thesis, 1988.

[22] J. L. Lions. *Some methods in the mathematical analysis of systems and their control*. Science Press, Beijing, China, 1981.

[23] J.P. Longley. A review of nonsteady flow models for compressor stability. *ASME Journal of Turbomachinery*, 116:202–215, 1994.

[24] C. A. Mansoux, D. L. Gysling, J. D. Setiawan, and J. D. Paduano. Distributed nonlinear modeling and stability analysis of axial compressor stall and surge. In *Proc. American Control Conference*.

[25] F.E. McCaughan. Bifurcation analysis of axial flow compressor stability. *SIAM Journal of Applied Mathematics*, 50:1232–1253, 1990.

[26] I. Mezić. A large-scale theory of axial compression system dynamics. *To appear in Journal of Fluid Dynamics*, 2000.

[27] F.K. Moore. A theory of rotating stall of multistage axial compressors: Part 1 - Small disturbances. *Transactions ASME Journal of Engineering for Gas Turbines and Power*, 106:313–320, 1984.

[28] F.K. Moore. A theory of rotating stall of multistage axial compressors: Part 2 - Finite disturbances. *Transactions ASME Journal of Engineering for Gas Turbines and Power*, 106:321–326, 1984.

[29] F.K. Moore. A theory of rotating stall of multistage axial compressors: Part 3 - Limit cycles. *Transactions ASME Journal of Engineering for Gas Turbines and Power*, 106:327–336, 1984.

[30] F.K. Moore and E.M. Greitzer. A theory of post-stall transients in axial compression systems: Part 1 - Development of equations. *Transactions ASME Journal of Engineering for Gas Turbines and Power*, 108:68–76, 1986.

[31] F.K. Moore and E.M. Greitzer. A theory of post-stall transients in axial compression systems: Part 2 - Application. *Transactions ASME Journal of Engineering for Gas Turbines and Power*, 108:231–239, 1986.

[32] Norbert Peters. *Turbulent Combustion*. Cambridge University Press, 2000.

[33] R.Temam. *"The Navier-Stokes Equations"*. Elsevier, Amsterdam, 1984.

[34] J. A. Sanders and F. Verhulst. *Averaging methods in nonlinear dynamical systems*, volume 59 of *Applied Math. Science*. Springer, New York, 1985.

[35] MQ Xiao and T. Basar. Analysis and control of multi-mode axial flow compression system models. *J. Dyn Syst. T, ASME*, 122(3):393–401, 2000.

[36] MQ Xiao and T. Basar. Center manifold of the viscous Moore-Greitzer pde model. *SIAM J. of Appl. Math.*, 61(3):855–869, 2000.